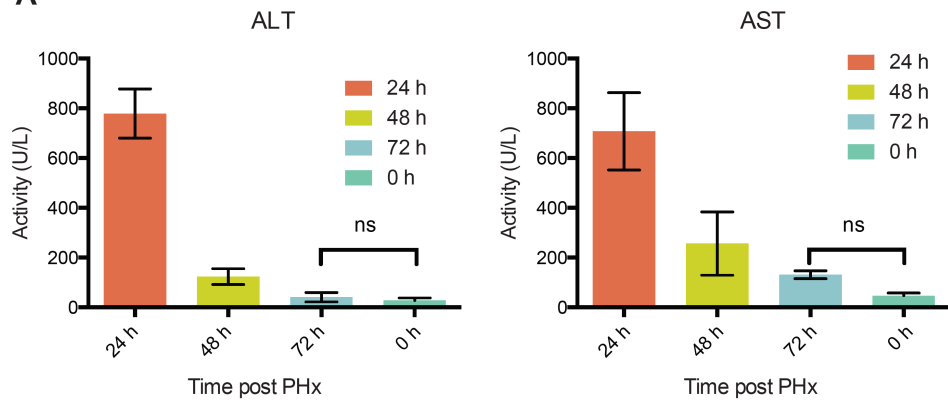
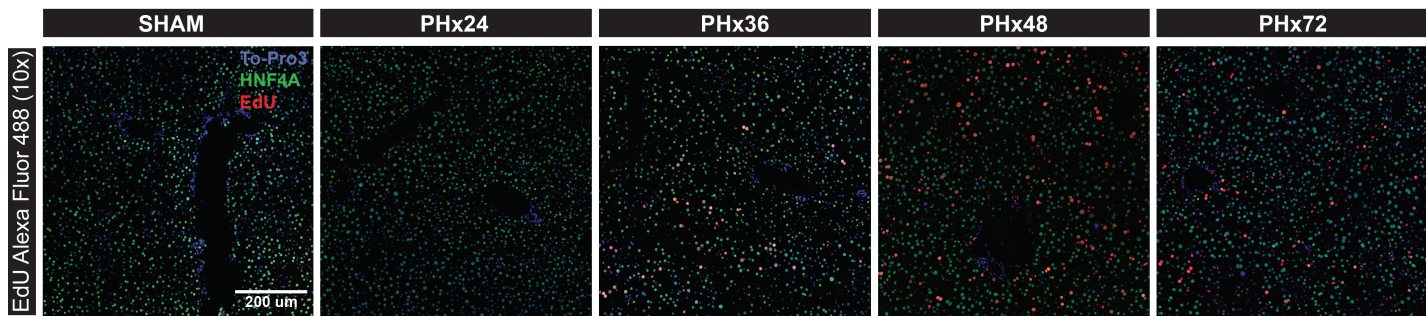
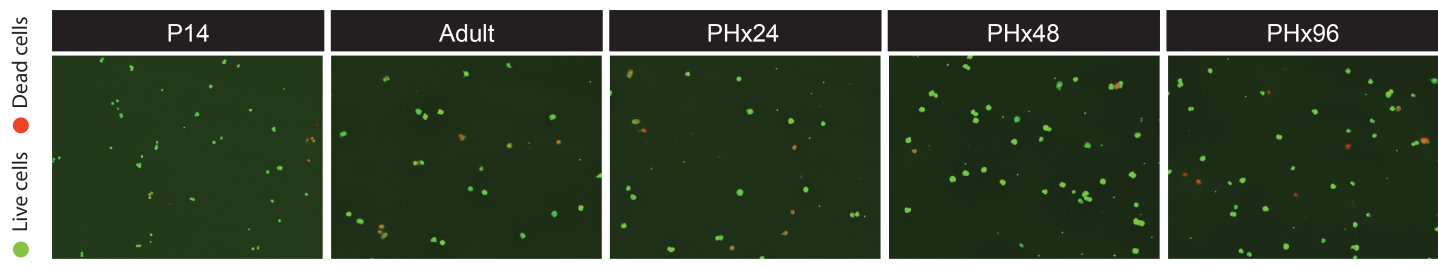
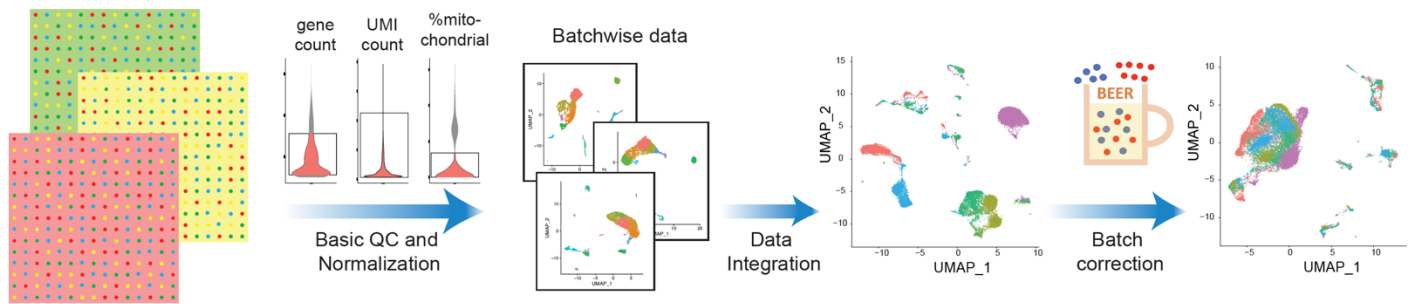


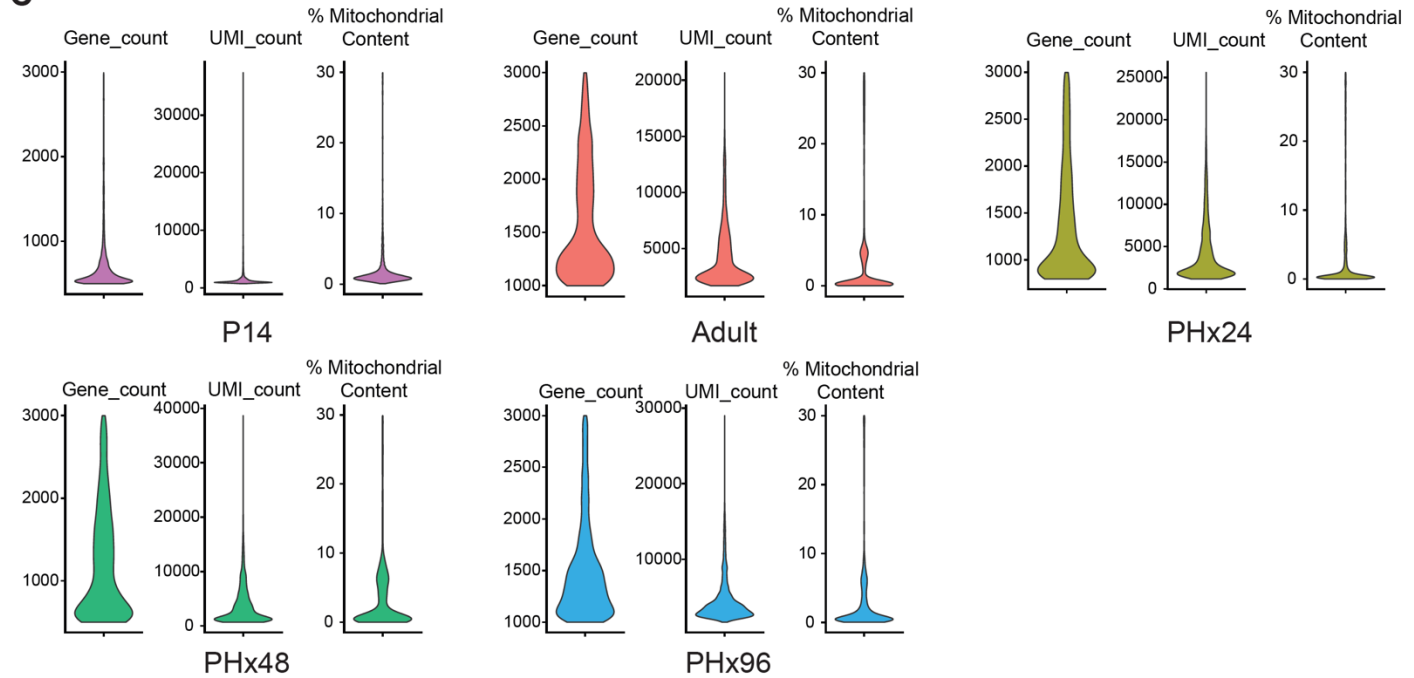
**A****B****C**

Viability :      83.1%      80.1%      87%      94.6%      89.1%

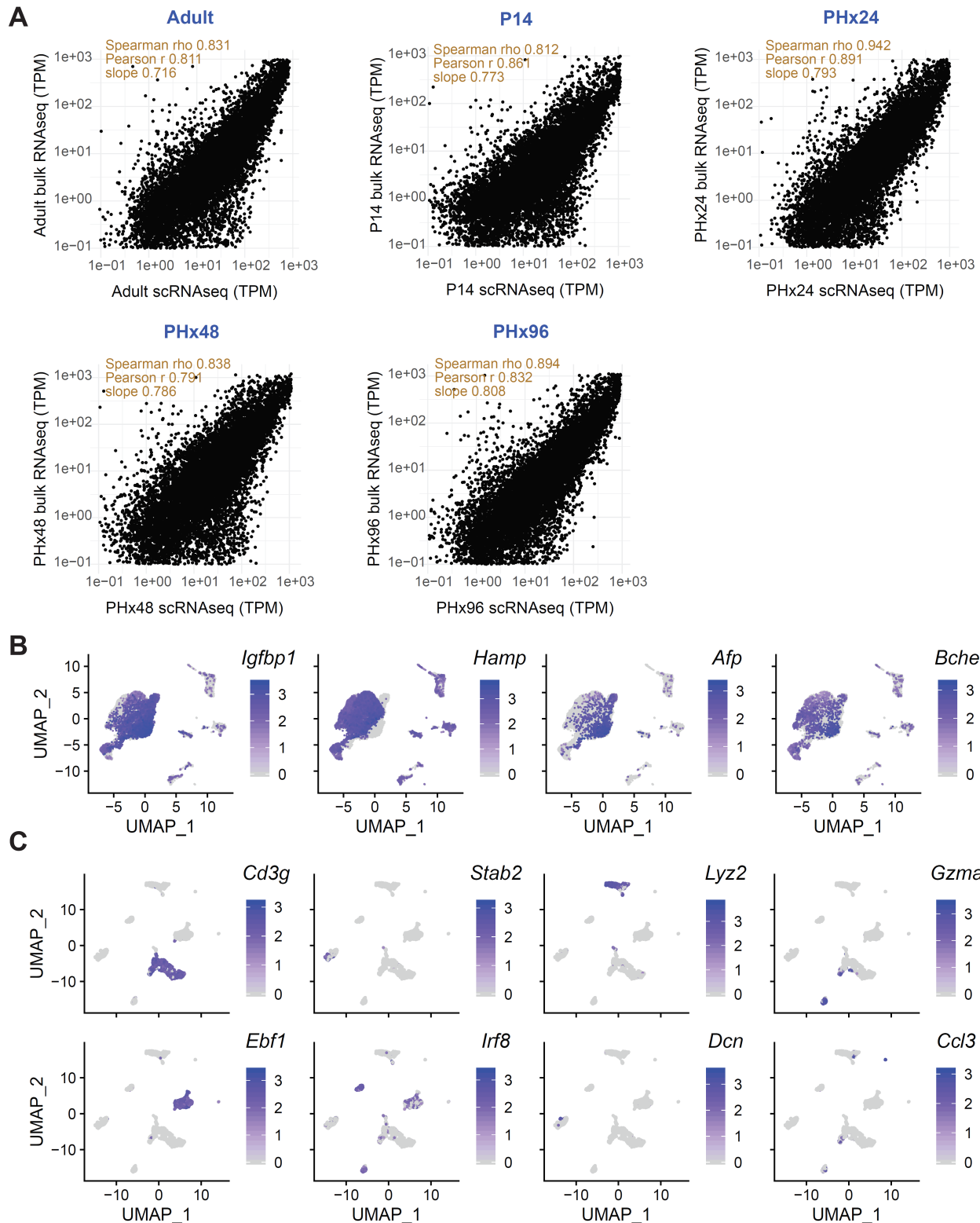
**Supplemental\_Fig\_S1:** **(A)** Levels of serum injury markers ALT and AST at 24, 48, and 72 h after PHx and at 0 h after SHAM surgeries. Both ALT and AST are restored to normal levels within 72 h after PHx. Data are mean  $\pm$  s.d. \*P < 0.05, ns: not significant, (n = 3 animals per group) **(B)** Fluorescent imaging of hepatocyte proliferation measured by *in vivo* EdU incorporation in livers following PHx or SHAM surgeries. White arrows indicate proliferating hepatocytes co-labeled for HNF4A (green), incorporated EdU (red), and nuclei (blue). **(C)** Fluorescent imaging of hepatocytes showing the viability of cells used for scRNA-seq. Dead/dying cells are stained in red (Propidium Iodide) and viable cells are stained in green (Acridine Orange). Percent viability calculated by Nexcelom Cellometer is also shown.

**A****B**

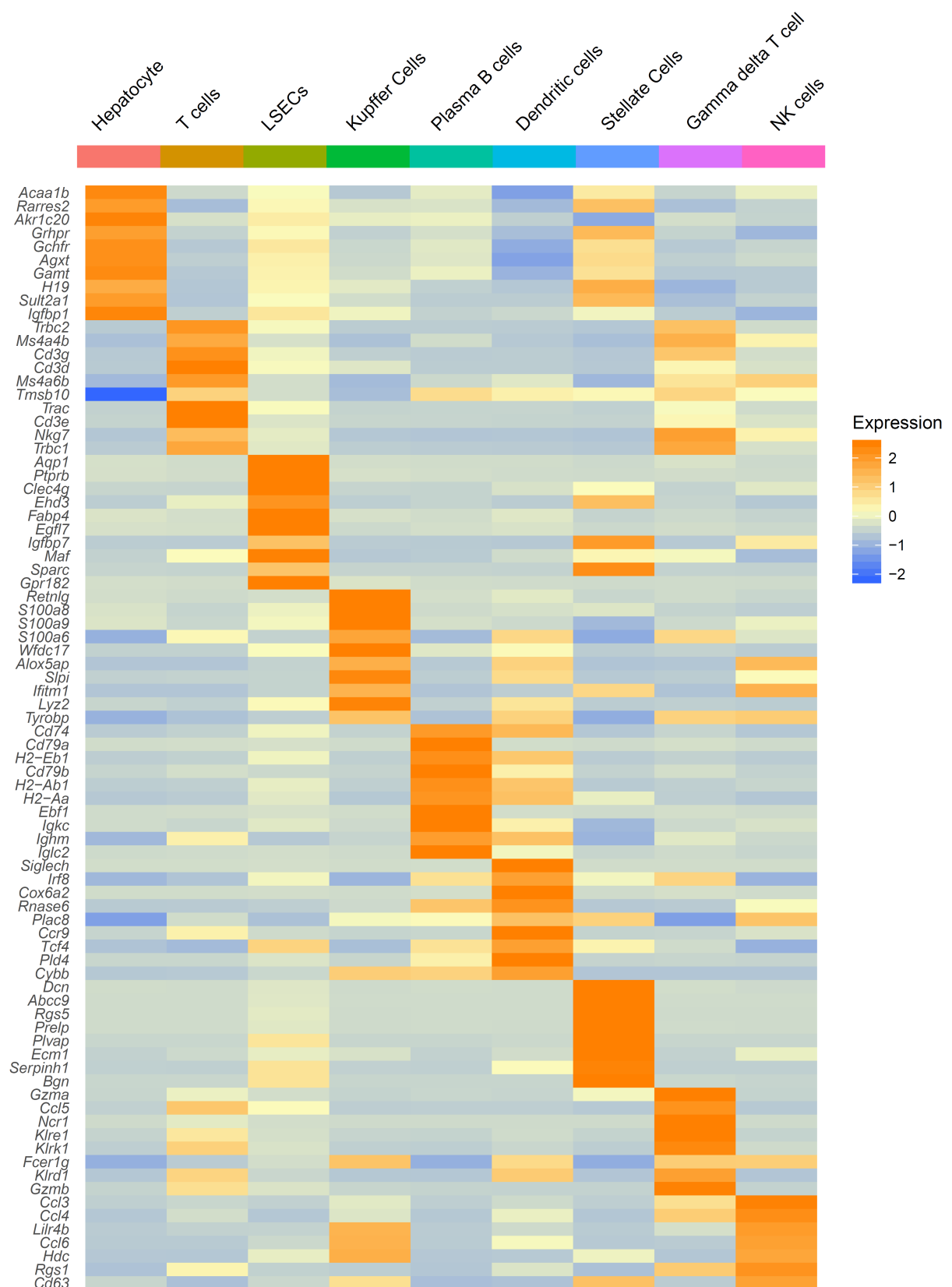
	Adult	PHx24	PHx48	PHx96	P14
Min cells	10	10	10	10	10
Min Features(genes)	1000	800	500	1000	500
Max Features(genes)	3000	3000	3000	3000	3000
% mitochondrial content	30	30	30	30	30

**C**

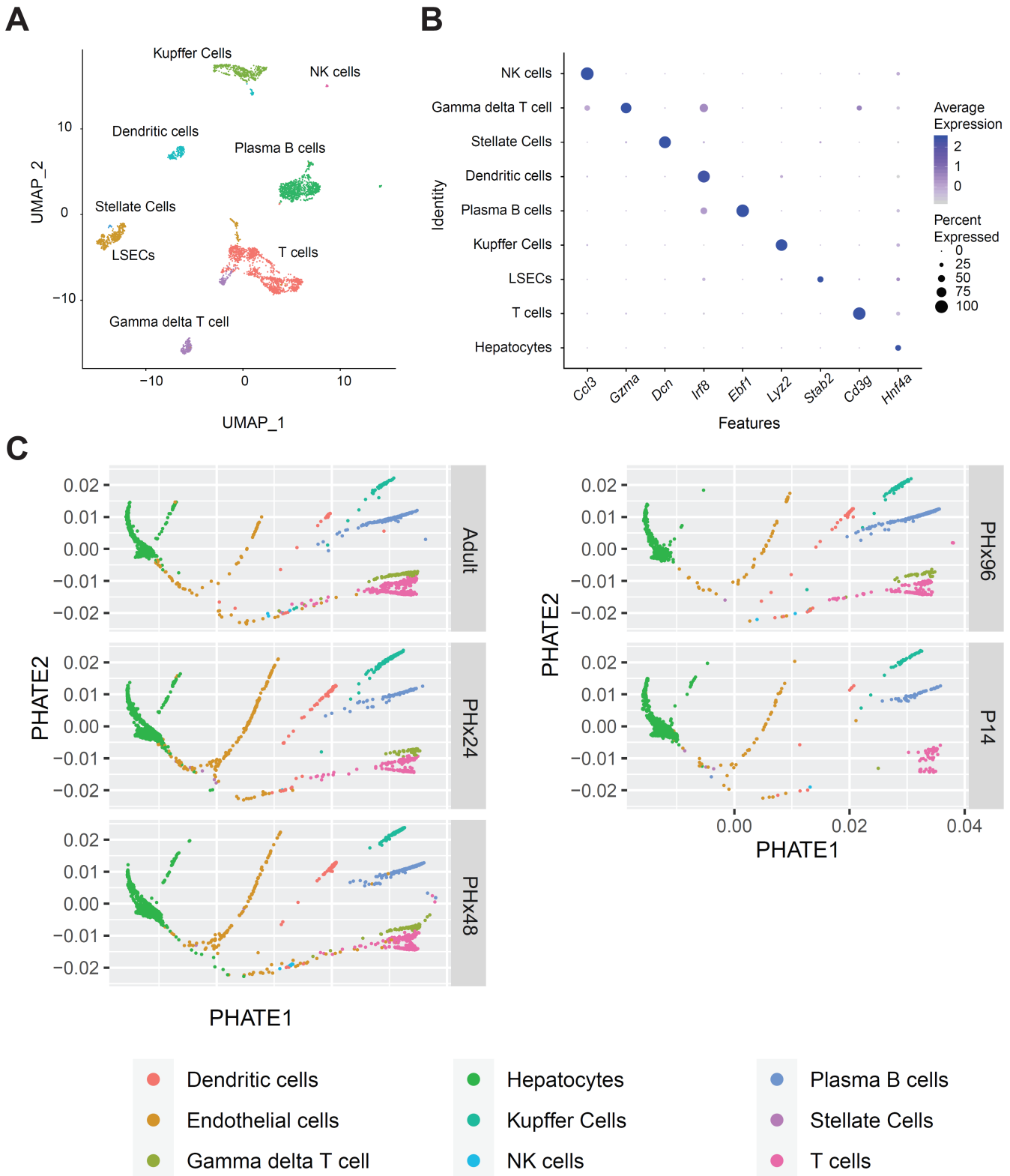
**Supplemental\_Fig\_S2:** **(A)** Computational workflow depicting data processing and analysis pipeline for scRNA-seq data. Cell Ranger was used to align the raw reads and generate feature-barcode matrices from scRNA-seq output for each sample. Seurat v3.1 was used to perform basic quality check (QC) and normalization, following which, the data was integrated using BEER to remove batch-specific effects. **(B)** Table showing the QC cutoffs applied on raw reads from scRNA-seq data prior to analysis. **(C)** Violin plots showing the distribution of gene counts, UMI counts and % mitochondrial content in P14, Adult, PHx24, PHx48 and PHx96 samples, after applying QC cutoffs.



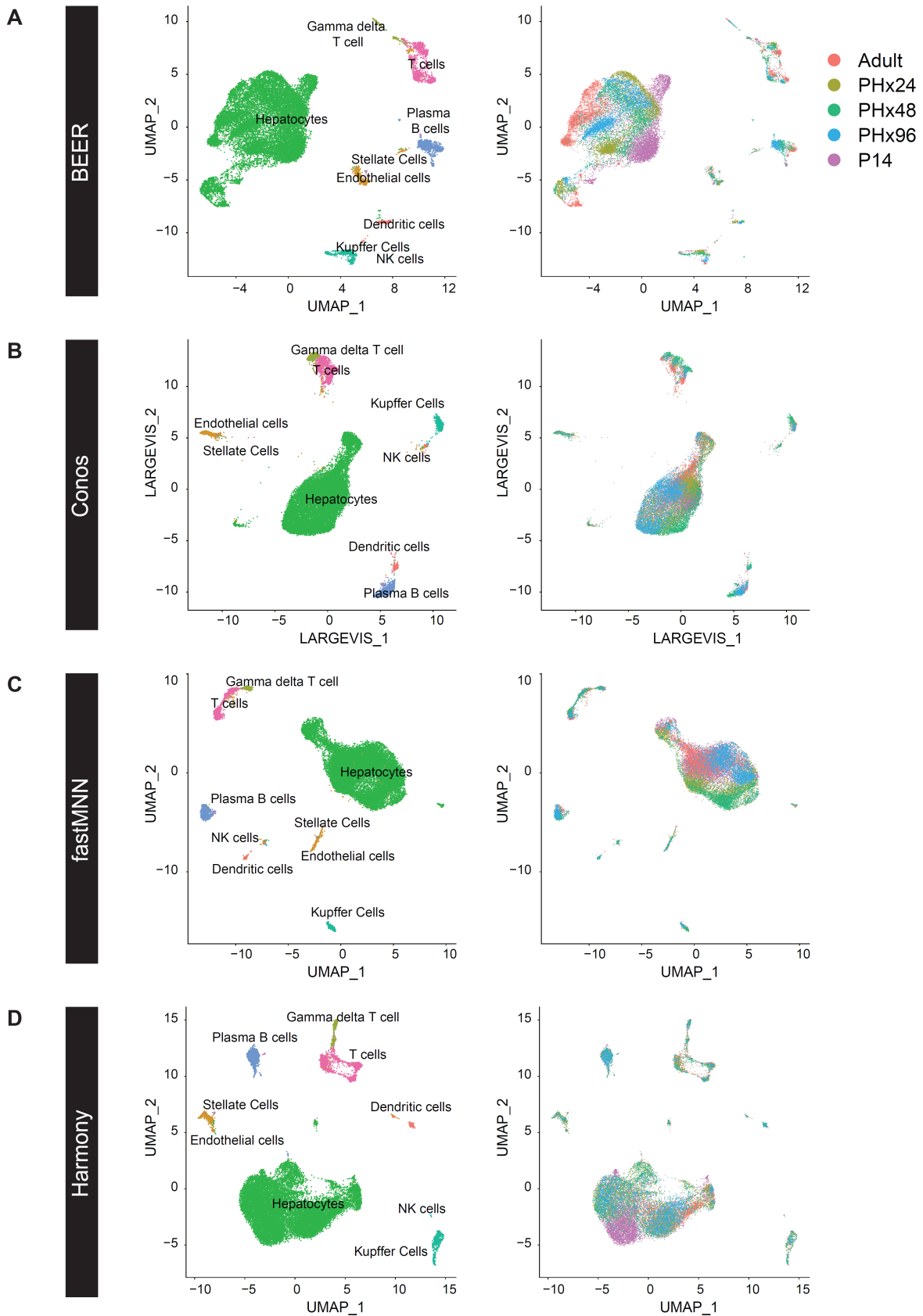
**Supplemental\_Fig\_S3:** **(A)** Scatter plots of gene expression (TPM) values comparing sc-RNAseq and bulk RNA-seq data at different time points of mouse liver maturation and regeneration. **(B)** UMAP plots representing the expression of hepatocyte-specific genes. **(C)** NPC subpopulation UMAP plots representing the expression of genes specific to different NPC populations identified. Cells in **B** and **C** are colored by the expression levels of the indicated gene, as calculated with Seurat v3.1.



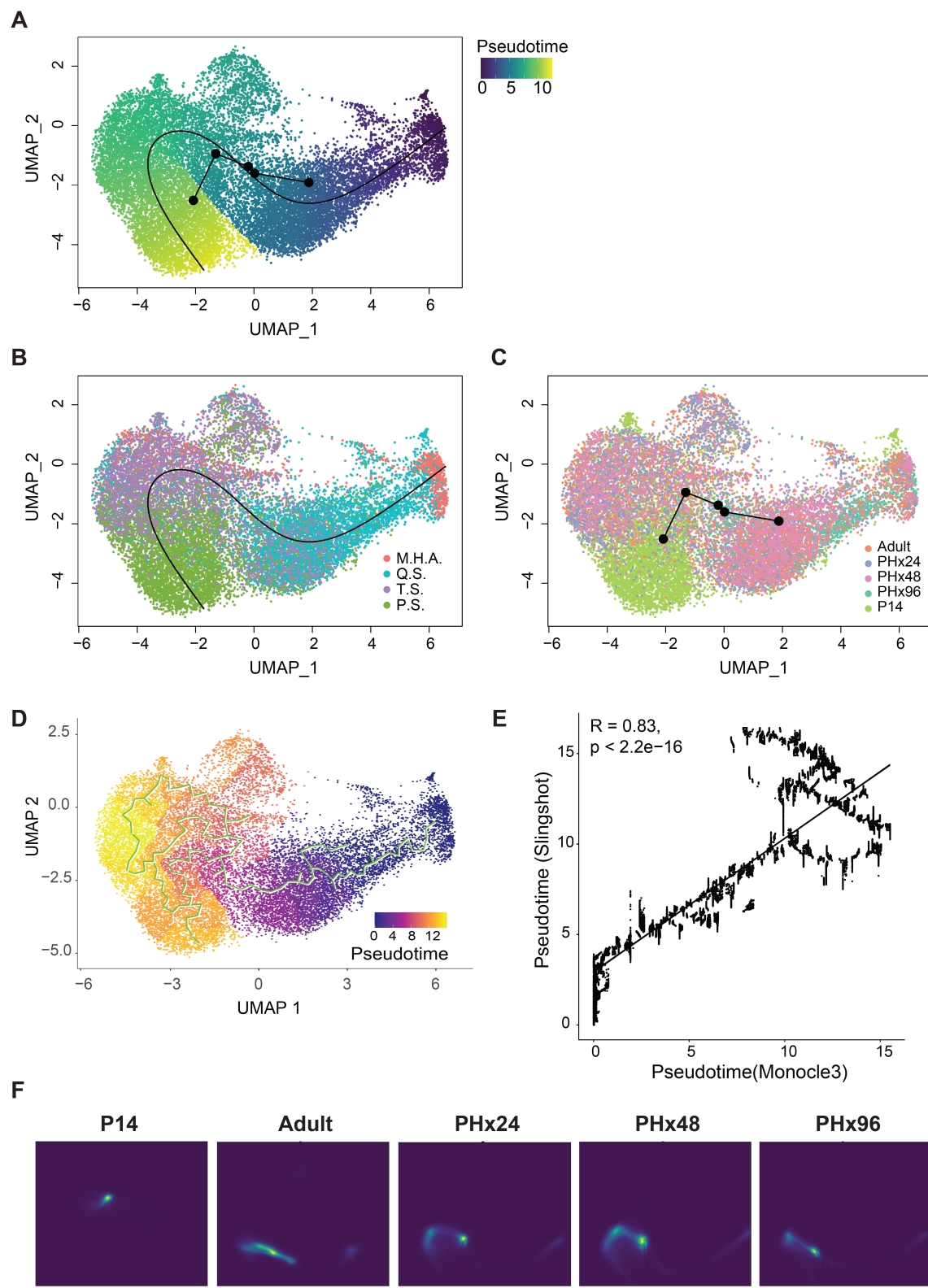
**Supplemental\_Fig\_S4:** Heatmap showing the relative expression of top genes that were enriched (>2 fold) within each cell type cluster. Scale bar depicts the color key of gene expression values plotted in the heatmap.



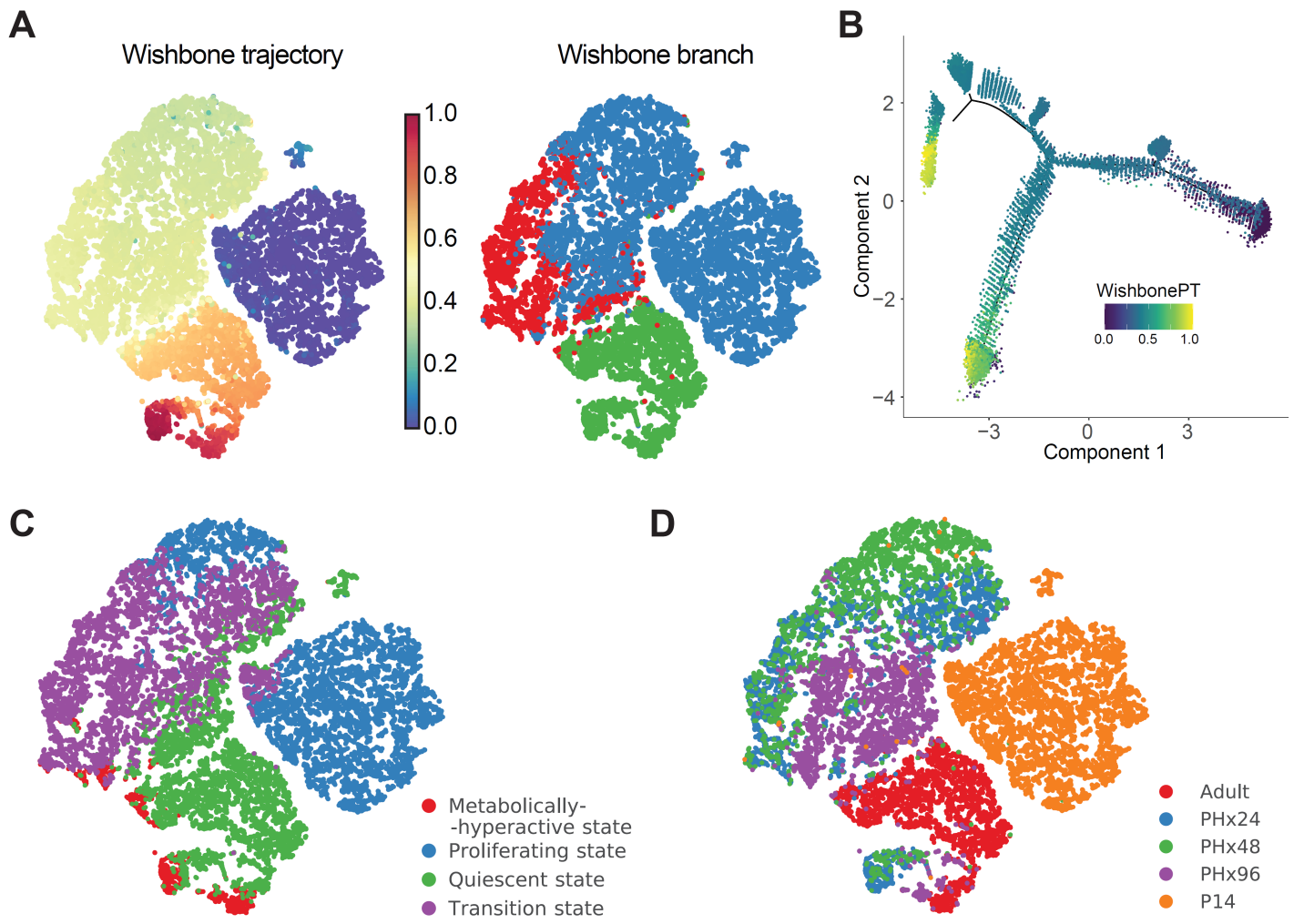
**Supplemental\_Fig\_S5:** **(A)** Combined UMAP projection of all NPC subpopulations. Analysis of known cell-specific marker genes revealed the identities of each cluster as a distinct NPC cell type **(B)** Dot plot showing expression of cell-type specific marker genes for each cell-type identified in the integrated dataset. The size of each dot encodes the percentage of cells expressing that marker within the identity class (cell type) and the color encodes the average expression of a gene among all cells within that class. **(C)** PHATE projection of cells separated by timepoints.



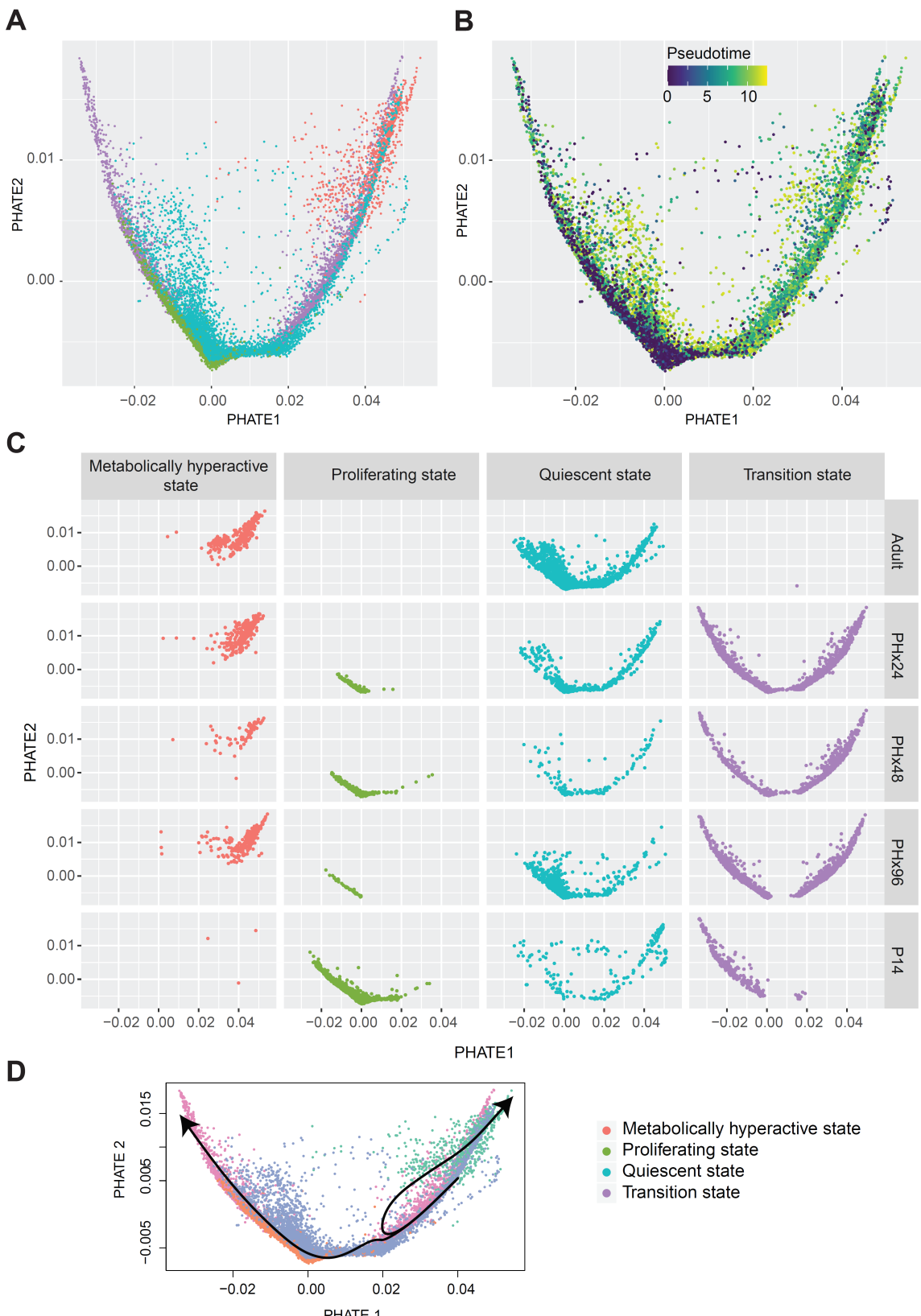
**Supplemental\_Fig\_S6:** Combined clustering of all 22,068 cells identified after QC cutoffs and batch correction using (A) BEER, (B) Conos (C) fastMNN and (D) Harmony. Cells are colored by the previously annotated cell type (left) and the batch of origin (right). Individual cell types grouped together after batch correction, demonstrating similar levels of correction success with each method.



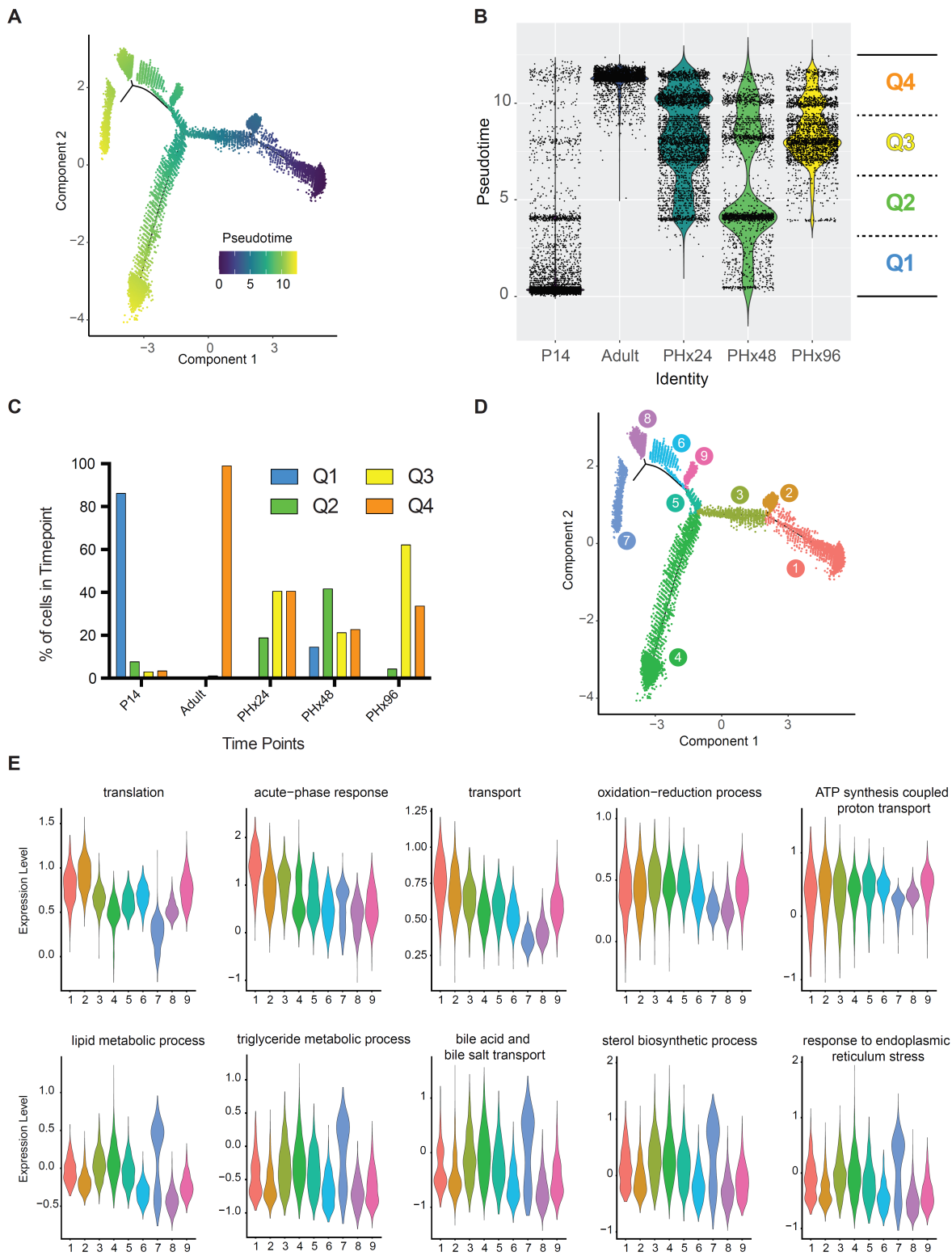
**Supplemental\_Fig\_S7:** Harmony corrected UMAP embeddings of hepatocytes colored by (A) slingshot derived pseudotime, (B) hepatocyte state, and (C) batch of origin. Nodes represent the five time points considered, with adult state as the starting node. The smooth line represents the smoothed trajectory over all points. (D) Harmony corrected UMAP embeddings of hepatocytes colored by pseudotime derived from Monocle3 and overlaid with Monocle 3 tree. (E) Correlation plot demonstrating concurrence of pseudotime values derived from Slingshot and Monocle3. (F) Snapshots of modeled Cell densities over five timepoints using TrajectoryNET.



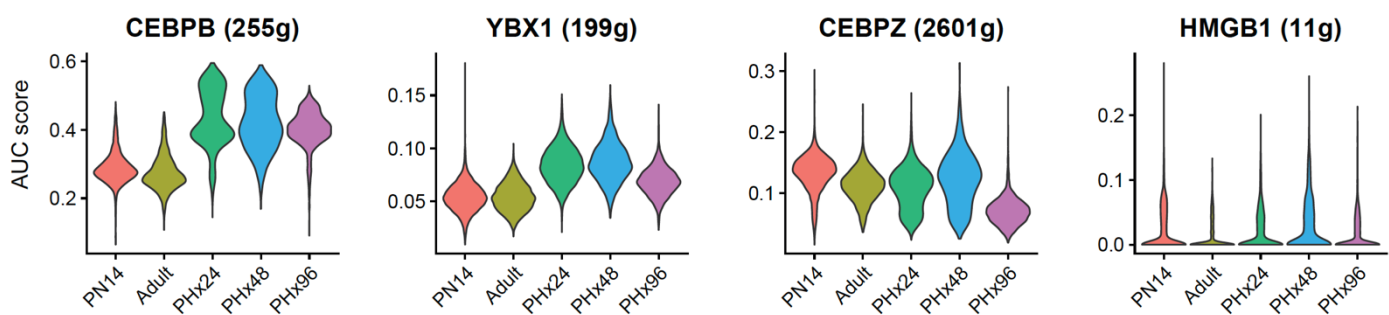
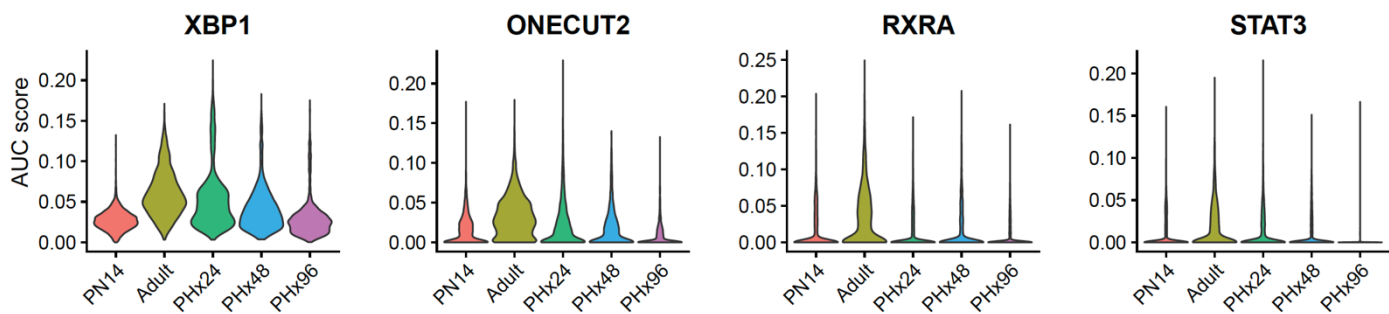
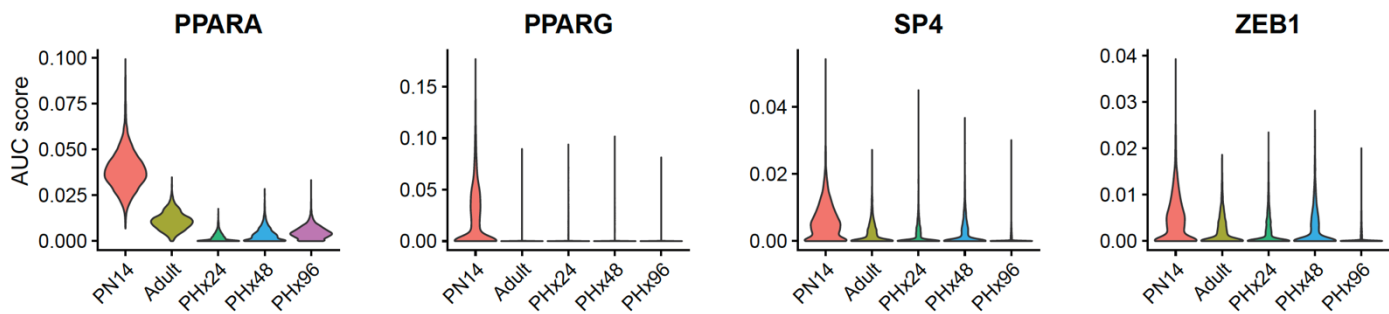
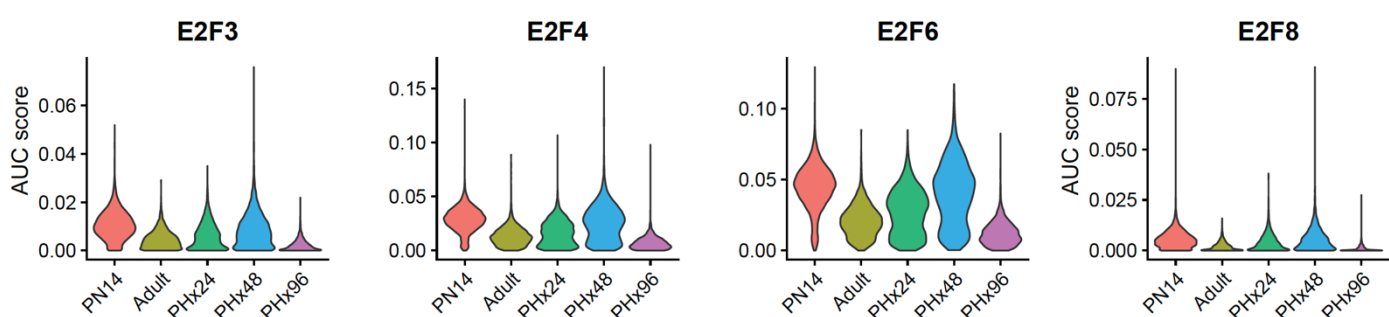
**Supplemental\_Fig\_S8:** **(A)** Wishbone derived trajectory (**left**) and branch associations (**right**) on BEER corrected t-SNE projection of hepatocytes. **(B)** WishbonePT values were plotted on the DDRTree trajectory derived from Monocle2 to show agreement between Monocle2 and WishBone. tSNE projection of hepatocytes with cells colored alternatively by **(C)** Cell State or **(D)** Sample timepoint identity. Wishbone orders the cells (transitioning from blue to red) with metabolically hyperactive cells and proliferating cells at the opposing ends of the trajectory. Metabolically hyperactive cells derived from PHx24 and PHx48 timepoints occupy the extreme ends of the trajectory.



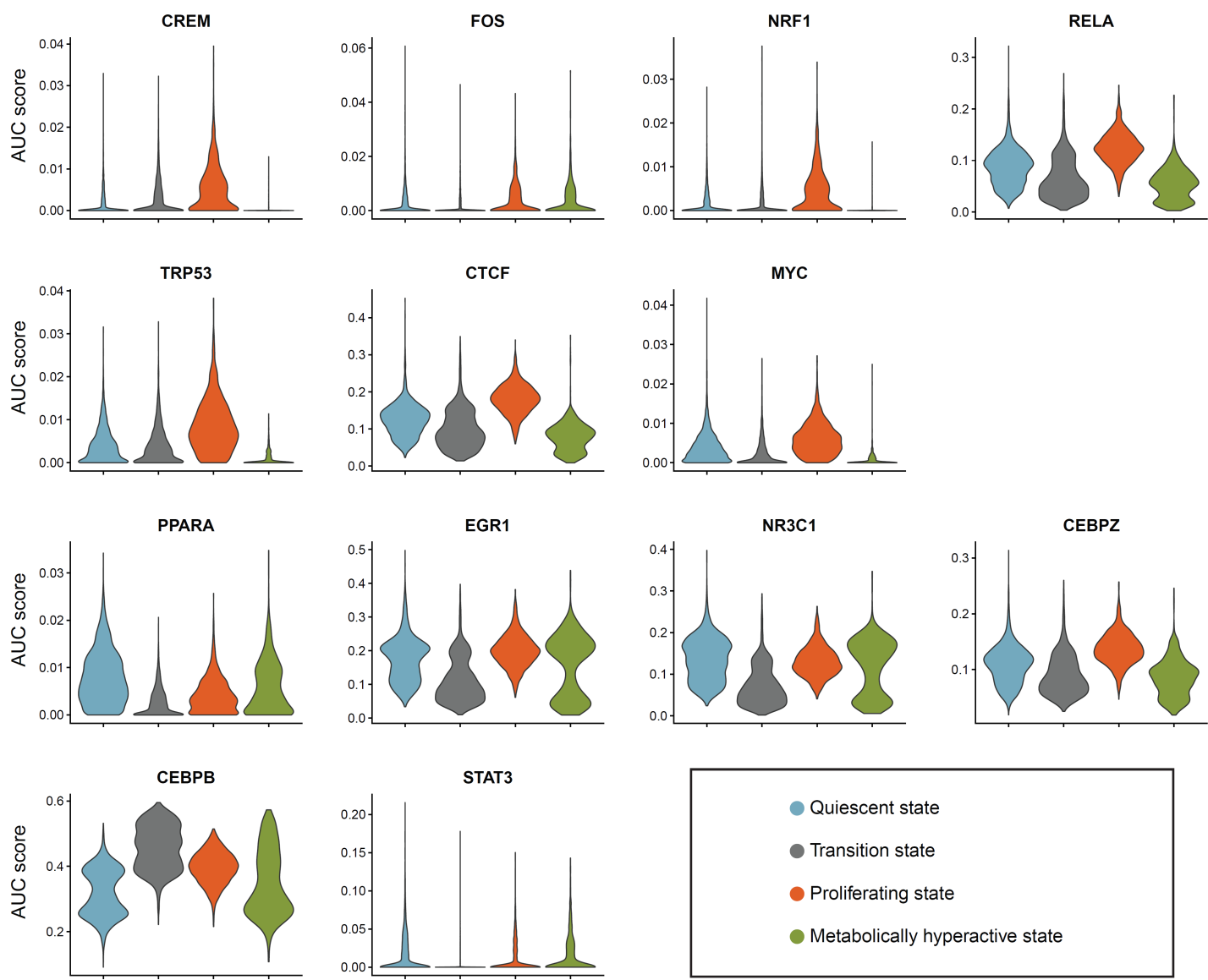
**Supplemental\_Fig\_S9:** FastMNN corrected PCA embeddings of hepatocytes represented in 2D space using PHATE projection. Cells are colored by **(A)** annotations as shown in Fig. 3 and **(B)** Pseudotime values derived from Monocle 2. **(C)** Cells are separated by the timepoint/sample they belong to and colored by the hepatocyte annotations. **(D)** Slingshot smoothed trajectory path over PHATE projection shows bifurcation towards the ends of the parabolic shape.



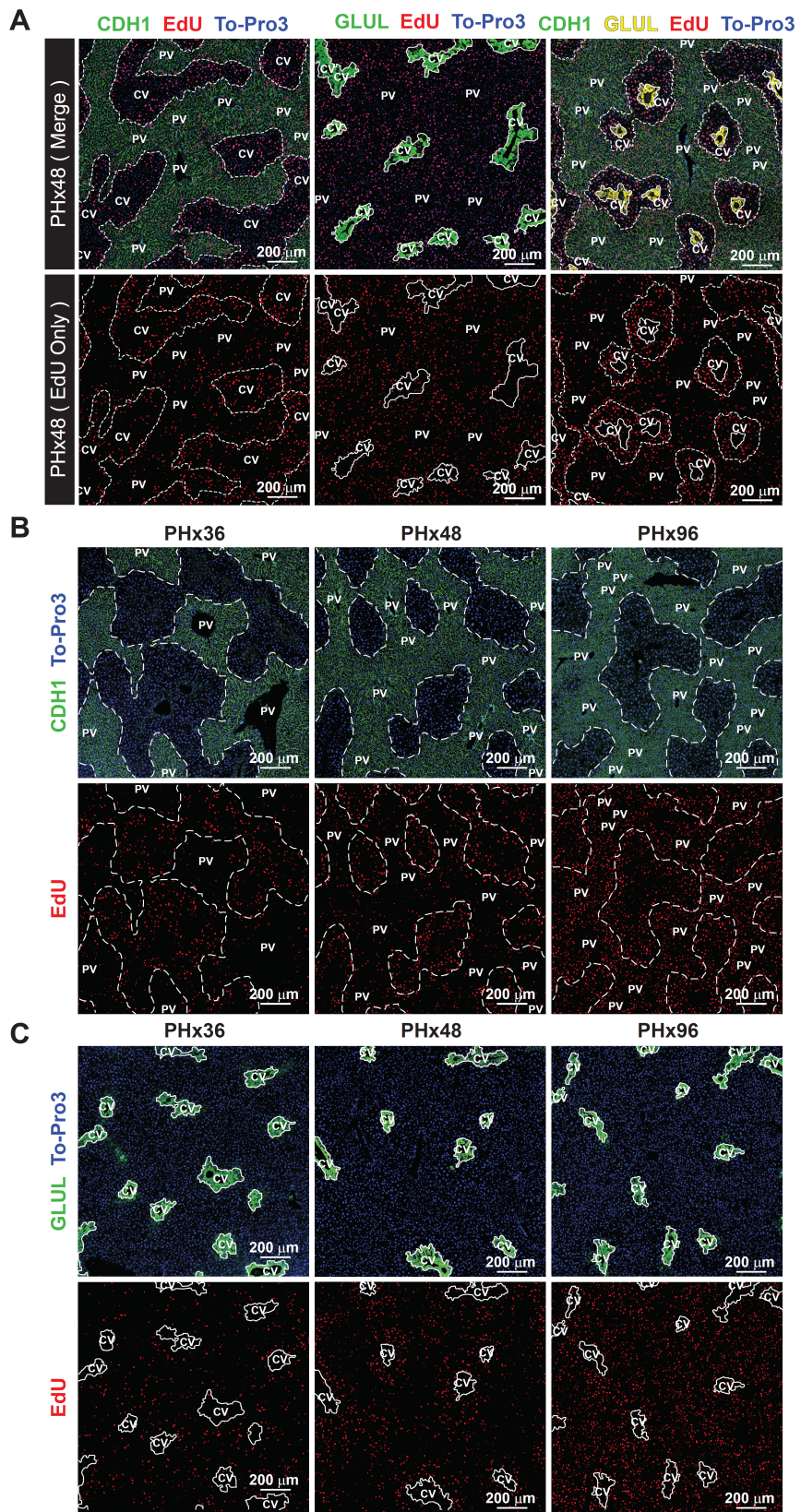
**Supplemental\_Fig\_S10:** **(A)** Pseudotime plot indicating cellular trajectories of hepatocytes from all samples. Trajectories are colored by pseudotime with P14 as the root state. **(B)** Violin plots showing the distribution of hepatocyte pseudotime values at individual time points. Pseudotime values were derived from Monocle 2 with P14 as the root. **(C)** Quartile distribution of Pseudotime values from B. **(D)** DDRTree trajectory showing the nine states identified by Monocle2 along the pseudotime trajectory for hepatocytes from all timepoints. **(E)** Violin plot showing relative scoring (from Seurat v3.1) for top ontology categories differentially regulated with respect to the trajectory bifurcation during regeneration for hepatocytes belonging to the cell states identified in D.

**A****Cluster-III****B****Cluster-IV****C****Cluster V****D**

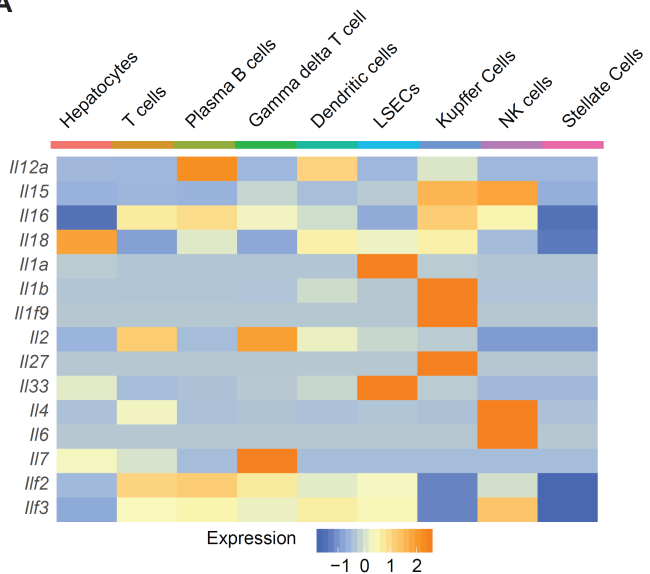
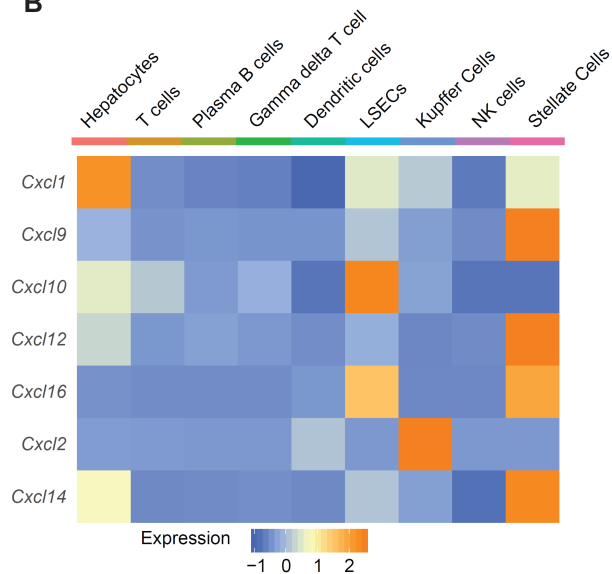
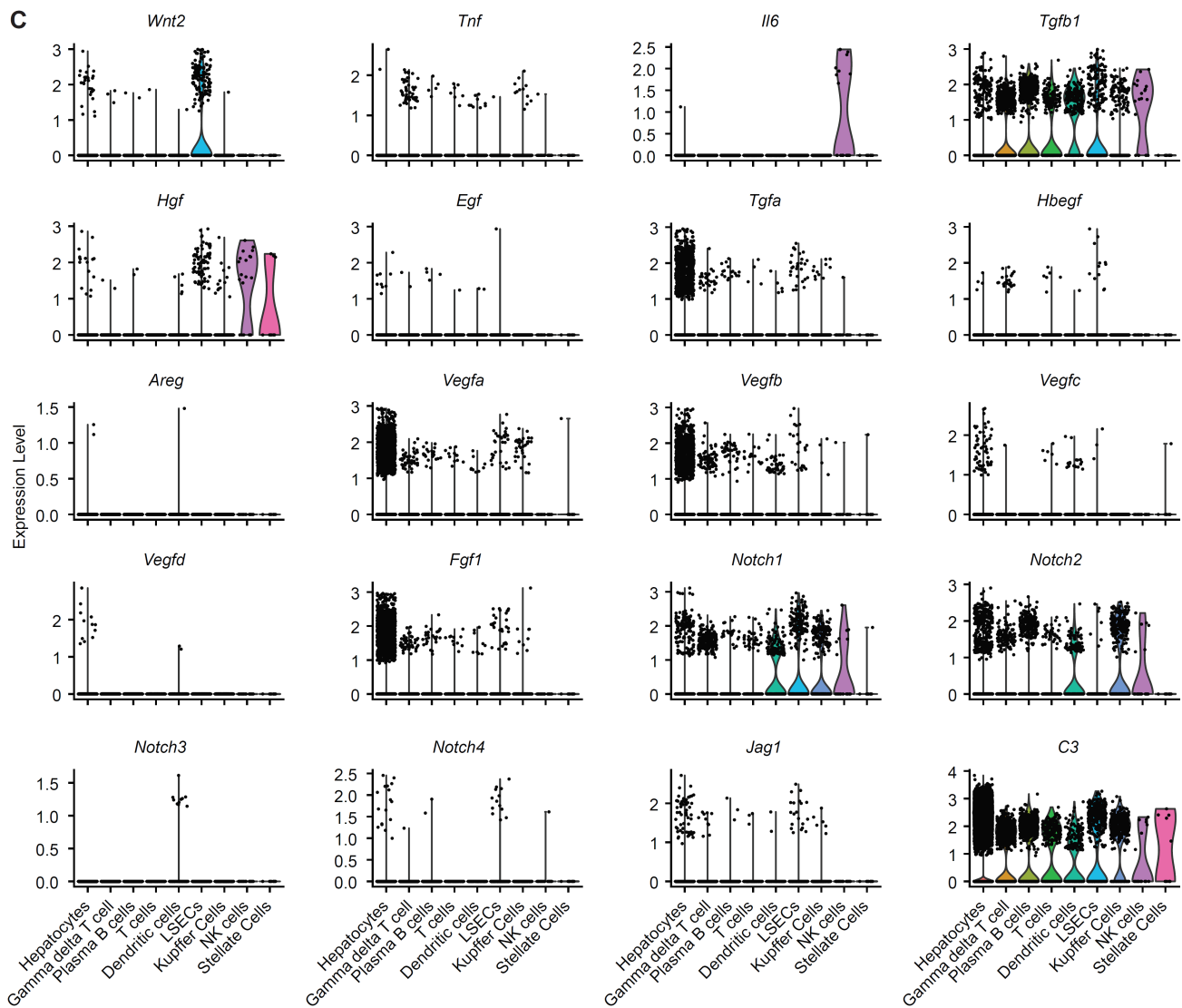
**Supplemental\_Fig\_S11:** Violin plots showing AUC-score distribution within hepatocytes at different time points, for the regulons belonging to **(A)** Cluster III **(B)** Cluster IV **(C)** Cluster V. **(D)** AUC-score distributions of regulon activities for various E2F transcription factors.



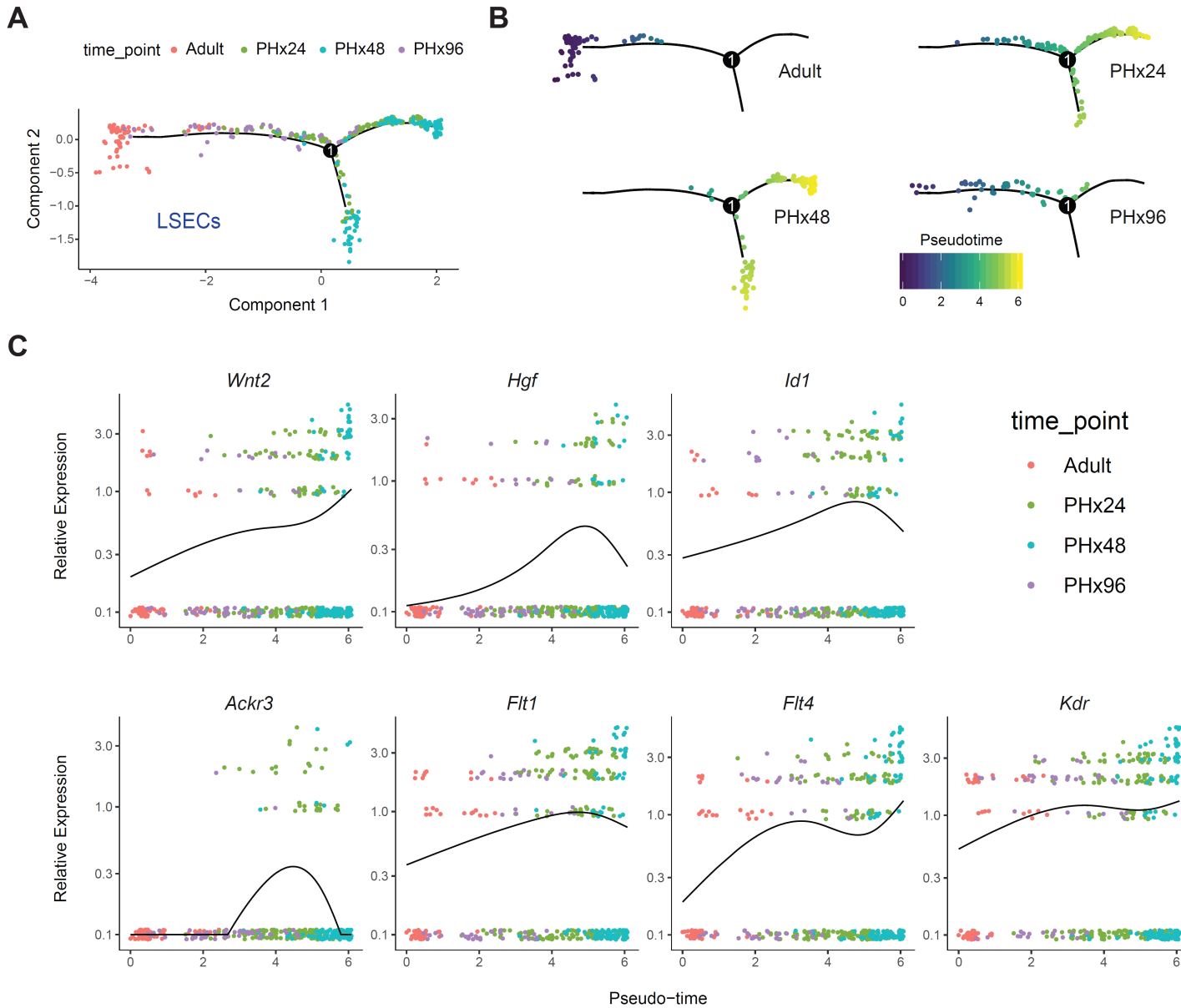
**Supplemental\_Fig\_S12:** Violin plots showing state-wise distribution of regulon activities (AUC-scores) in hepatocytes for various transcription factors.



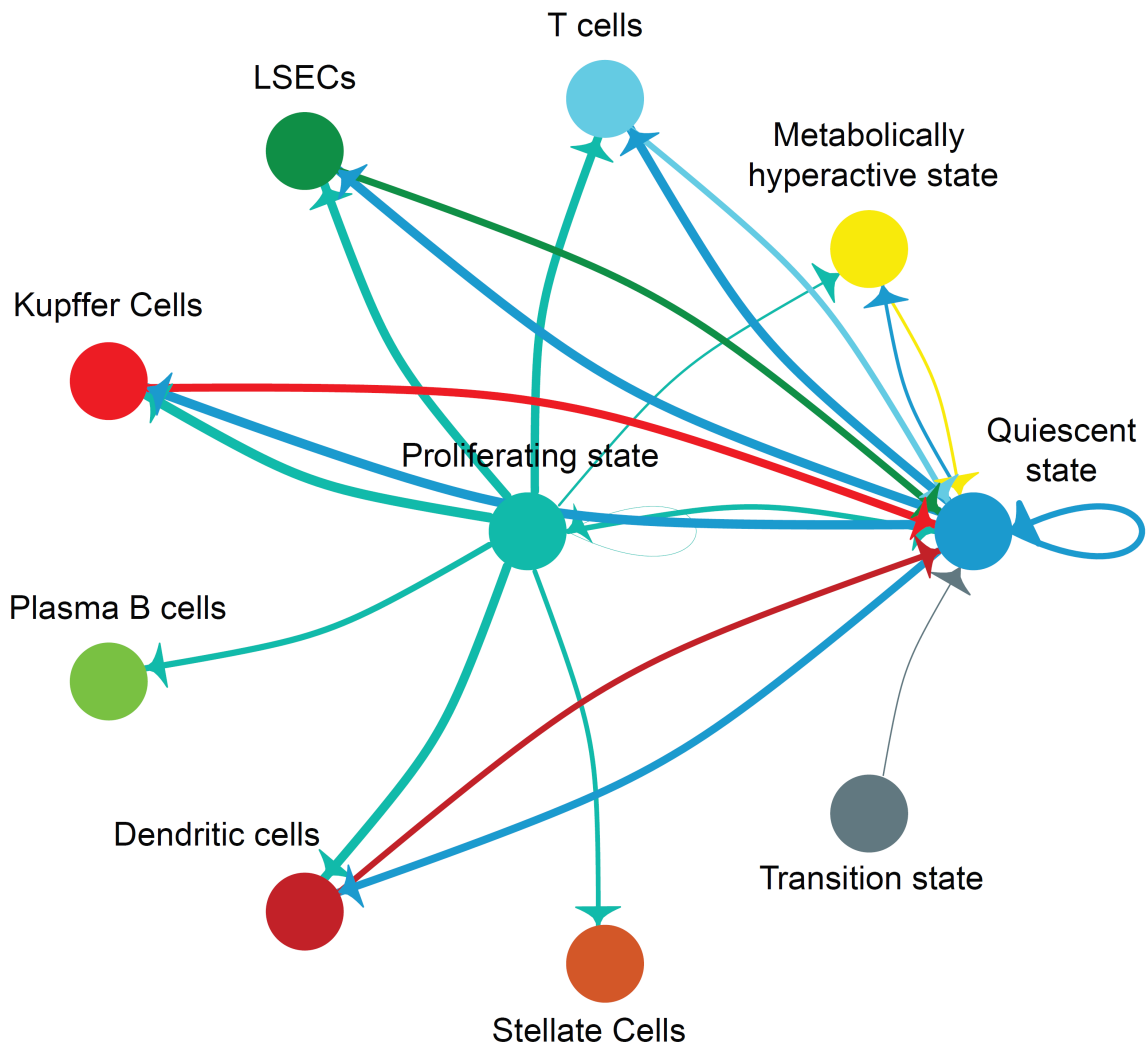
**Supplemental\_Fig\_S13:** Representative immunofluorescence images depicting spatial segregation of metabolic and proliferating hepatocytes. **(A)** Combined labeling of periportal (CDH1+) or pericentral (GLUL+) hepatocytes along with EdU at PHx48. **(B)** Periportal (CDH1+) or **(C)** Pericentral (GLUL+) hepatocytes co-labeled with EdU over time show that hepatocyte proliferation after PHx initiates in the midlobular region and proceeds towards the metabolically active periportal and pericentral areas.

**A****B****C**

**Supplemental\_Fig\_S14:** Heatmap demonstrating cell-type-specific expression patterns of **(A)** Interleukins and **(B)** Chemokines identified in the sRNA-seq datasets. **(C)** Violin Plots showing cell-type-specific expression patterns of different mitogens.

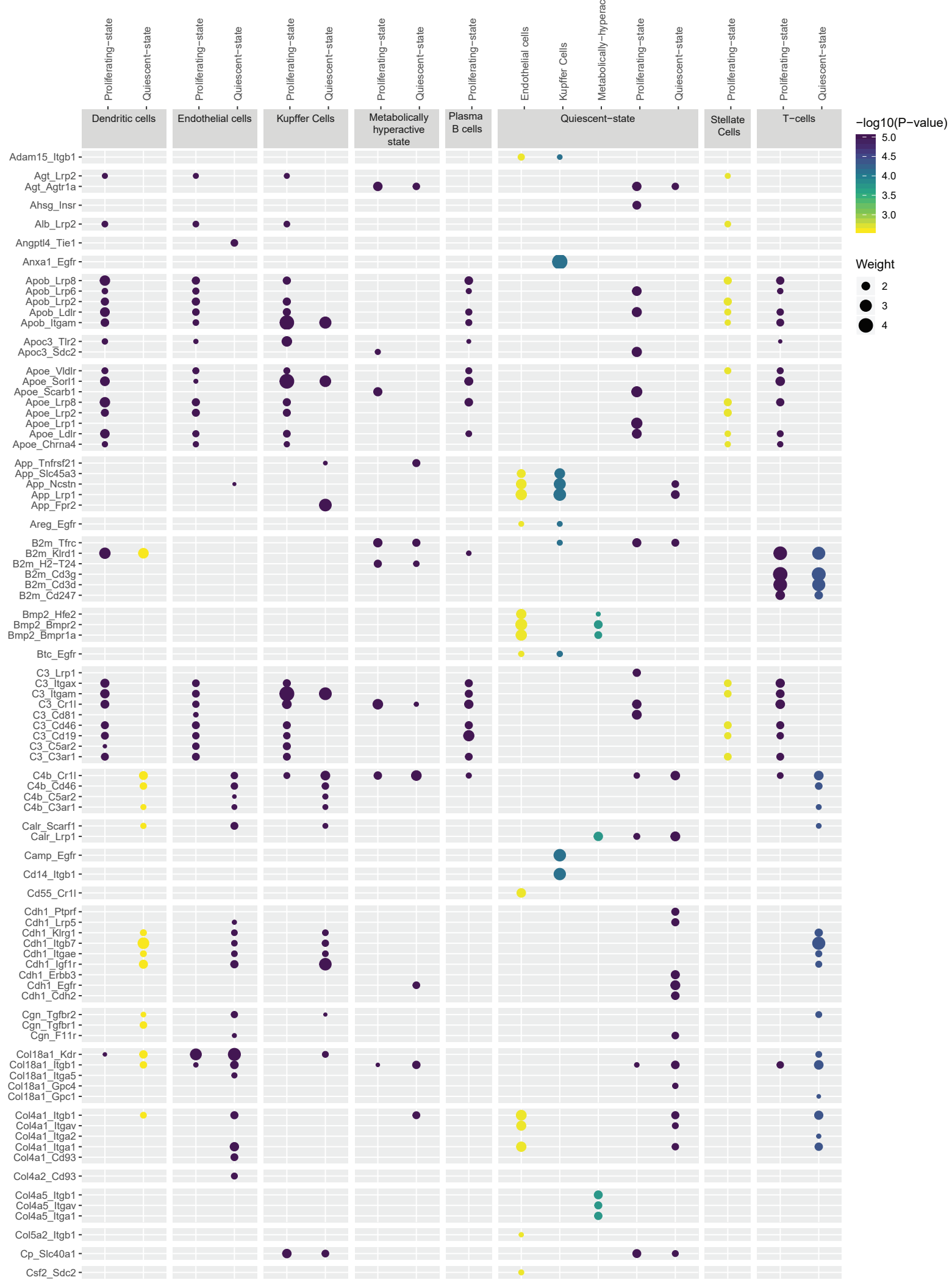


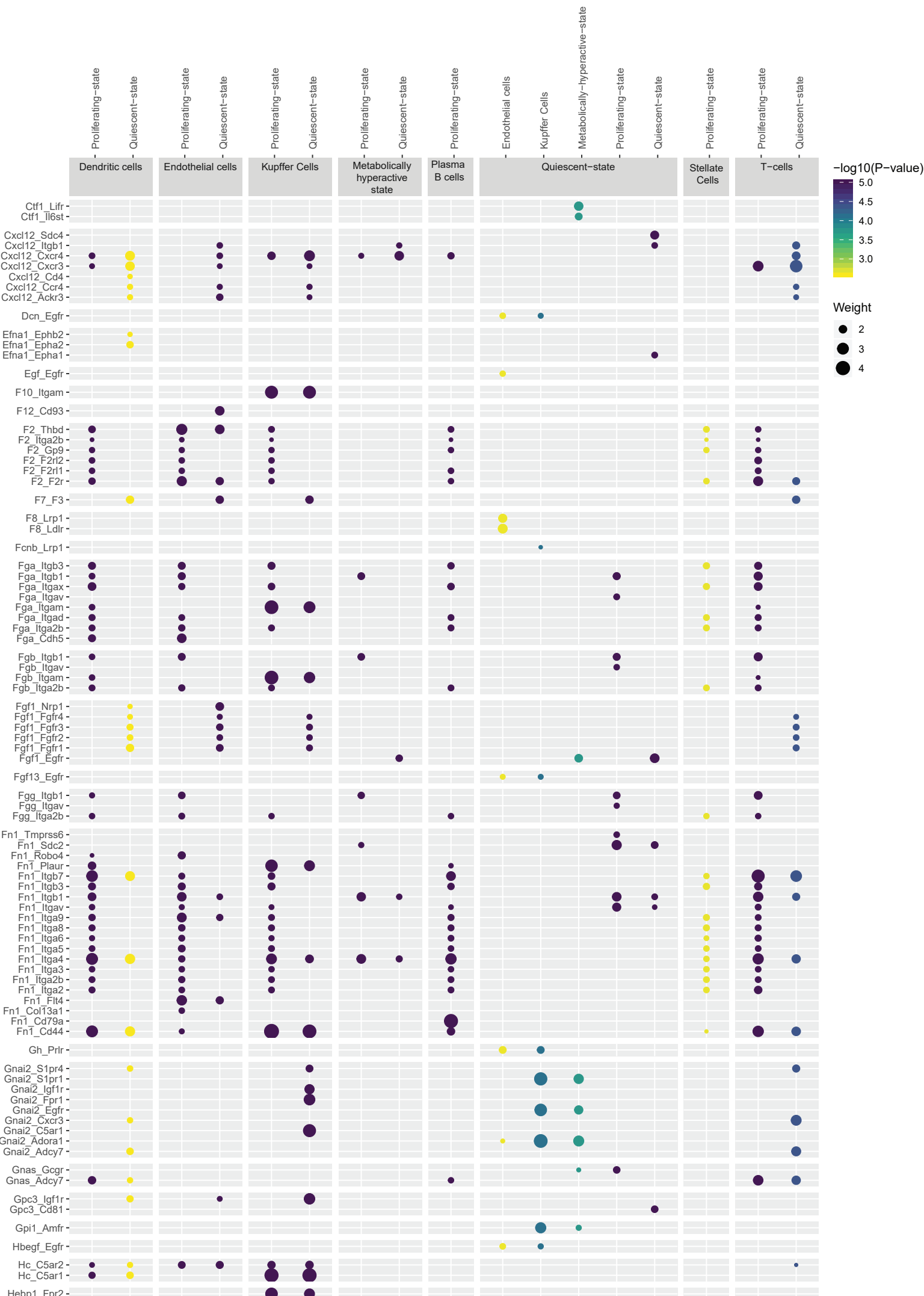
**Supplemental\_Fig\_S15:** (A) LSEC activation during regeneration. Single cell trajectories were constructed and pseudotime values were calculated using Monocle 2, with LSECs identified from Adult, PHx24, PHx48 and PHx96 samples. Cells within trajectories are colored by sample identity. (B) Distribution of LSECs from different time points along the activation trajectory. Cells are colored by pseudotime value. (C) Variation in relative expression levels of LSEC activation-associated genes along the pseudotime trajectory. X- and Y-axis correspond to the pseudo-time value for each cell and the relative expression level of a given gene respectively.

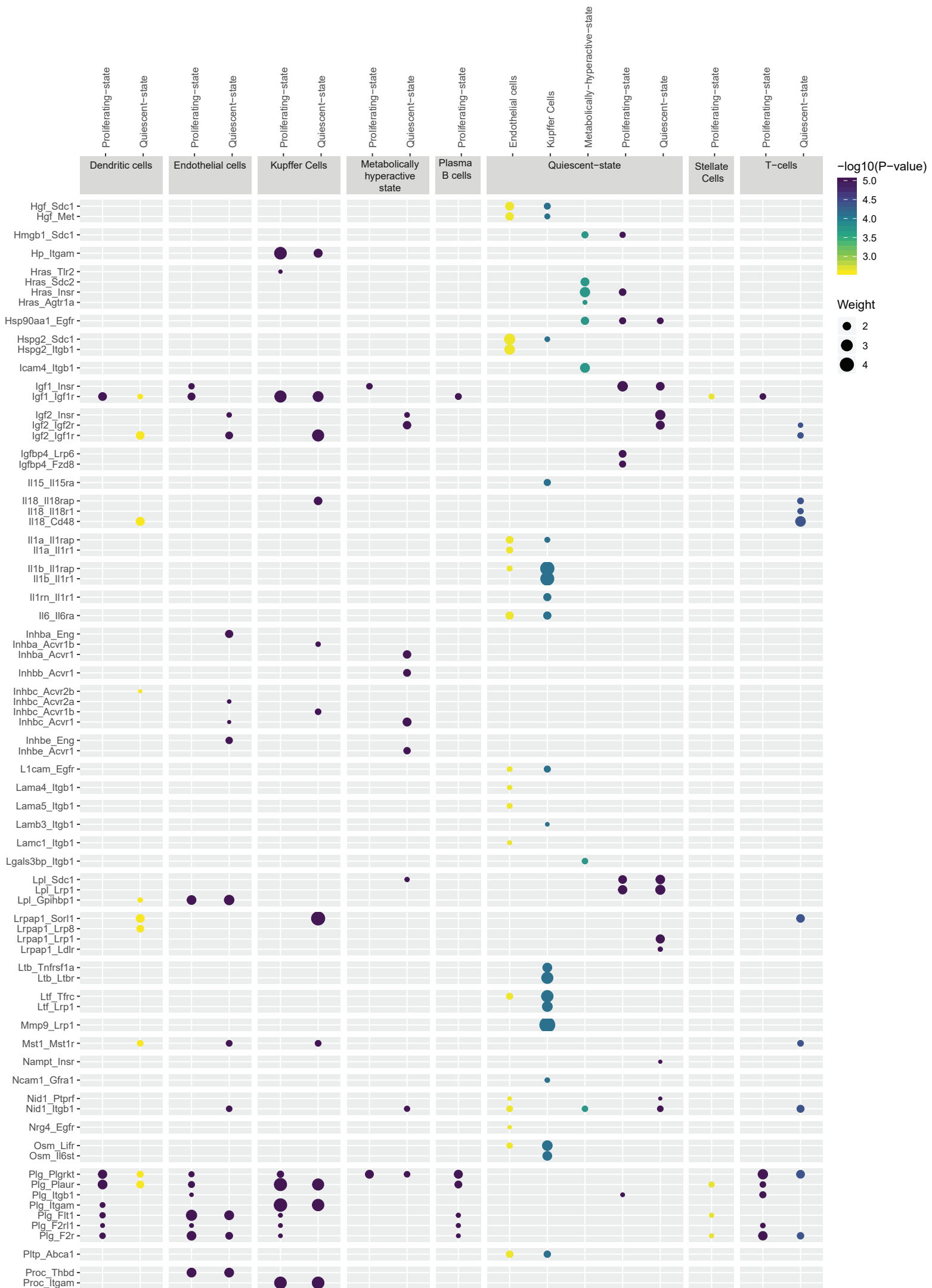


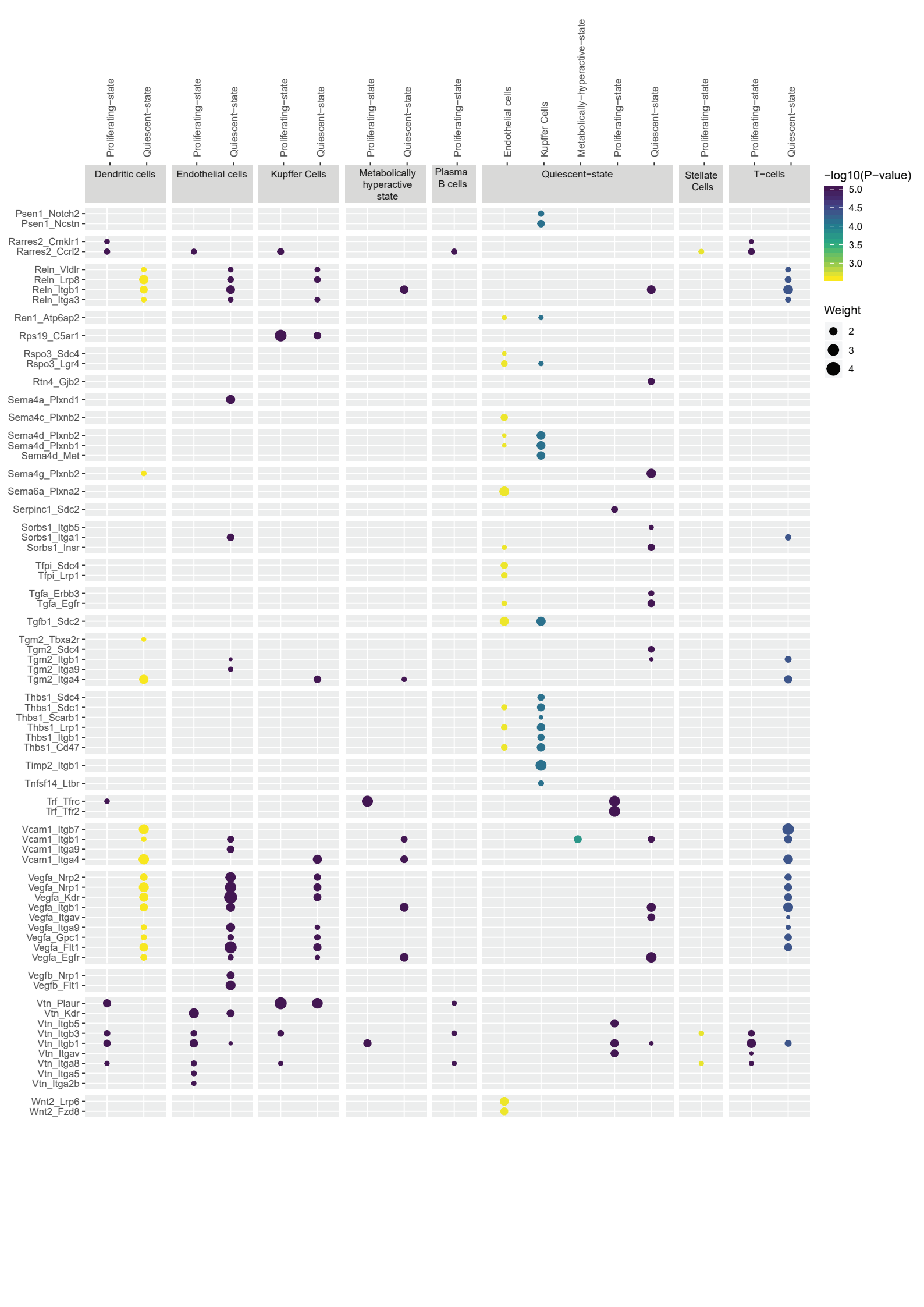
**Supplemental\_Fig\_S16:** Network diagram showing significant cell-cell interactions for P14. The interactions are indicated by arrows (edges) pointing in the source to target direction. Thickness indicates the sum of weighted paths between populations and the color of arrows corresponds to the source.

## Supplemental\_Fig\_S17: P14\_Ligand\_receptor\_interactions

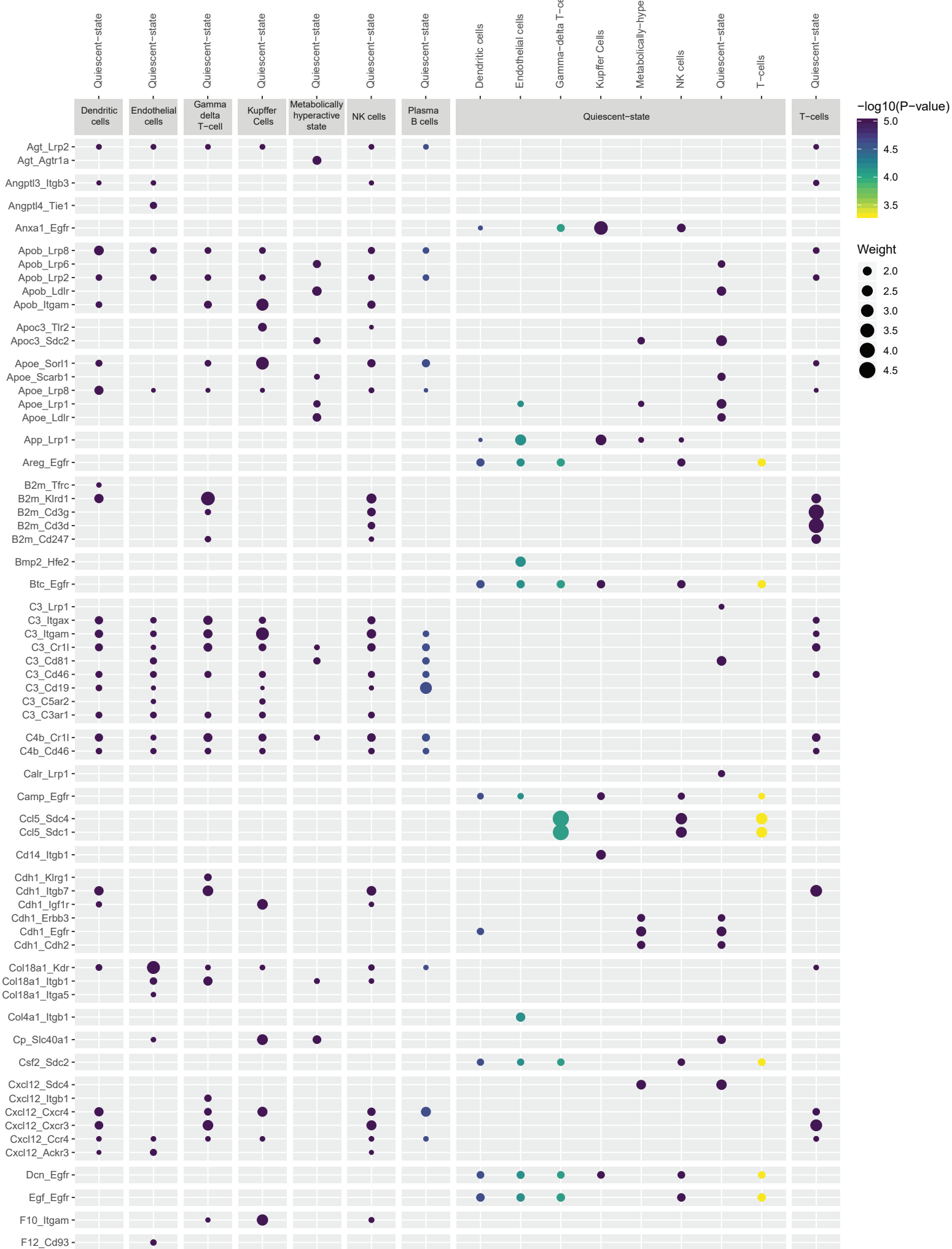


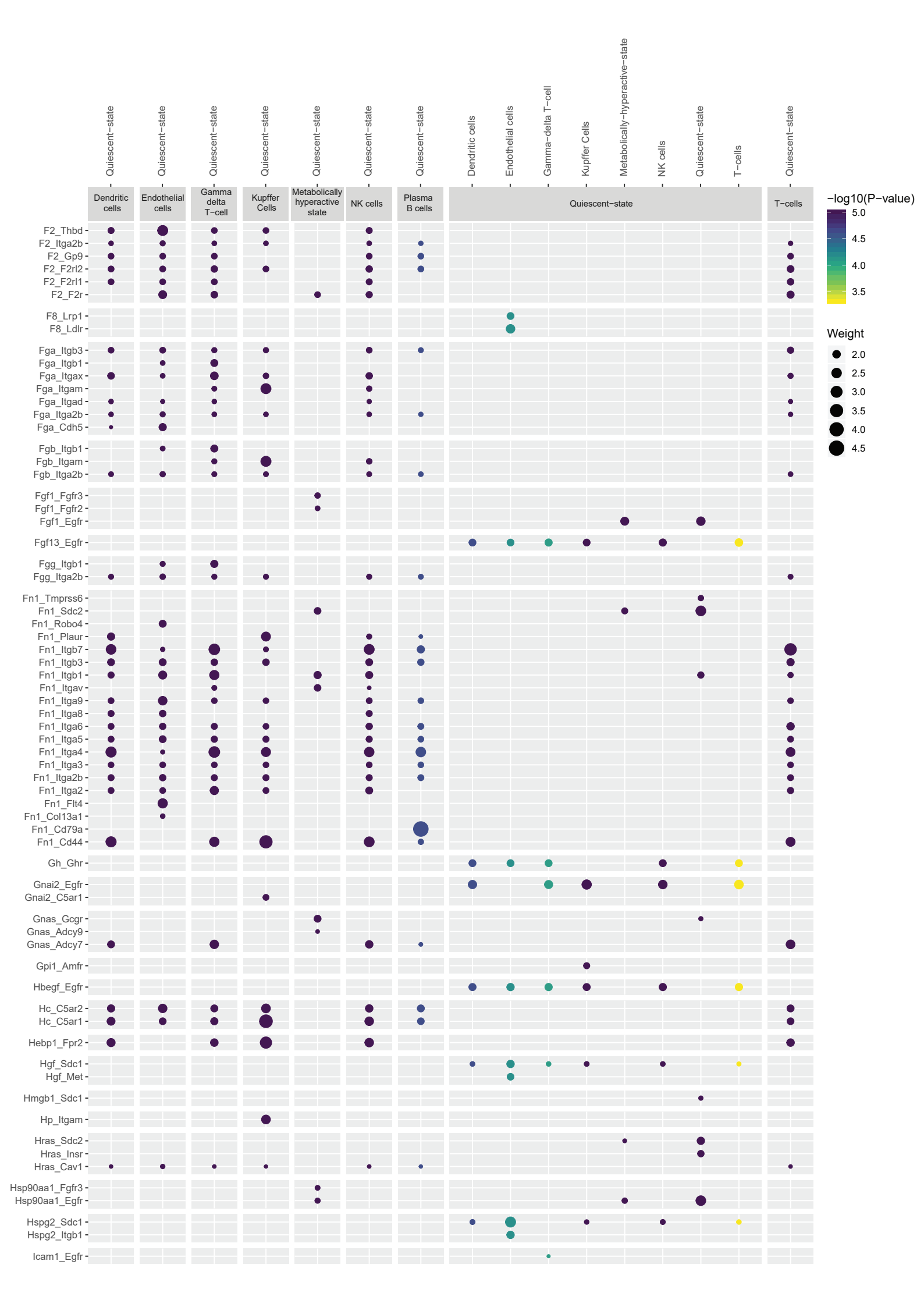


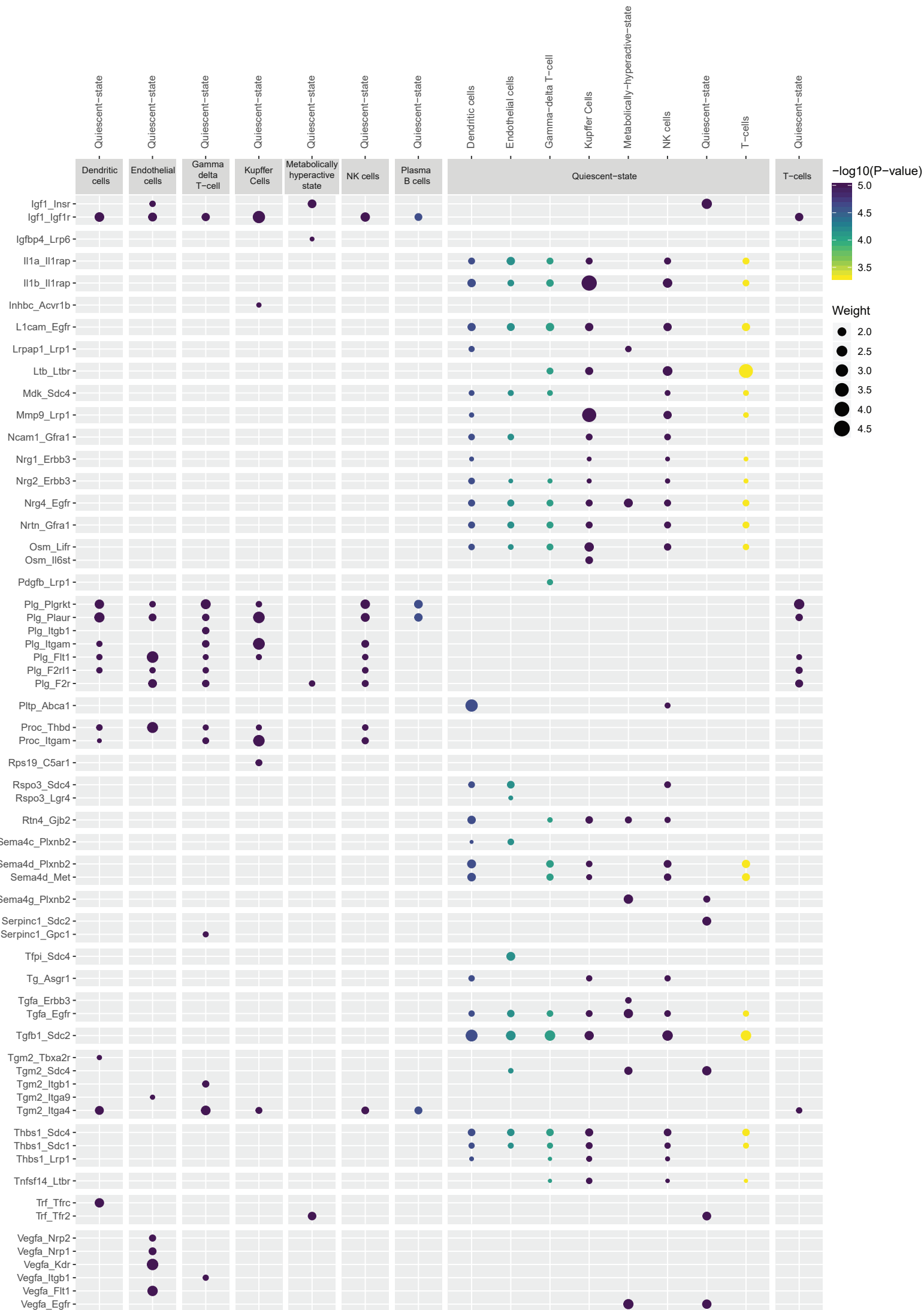


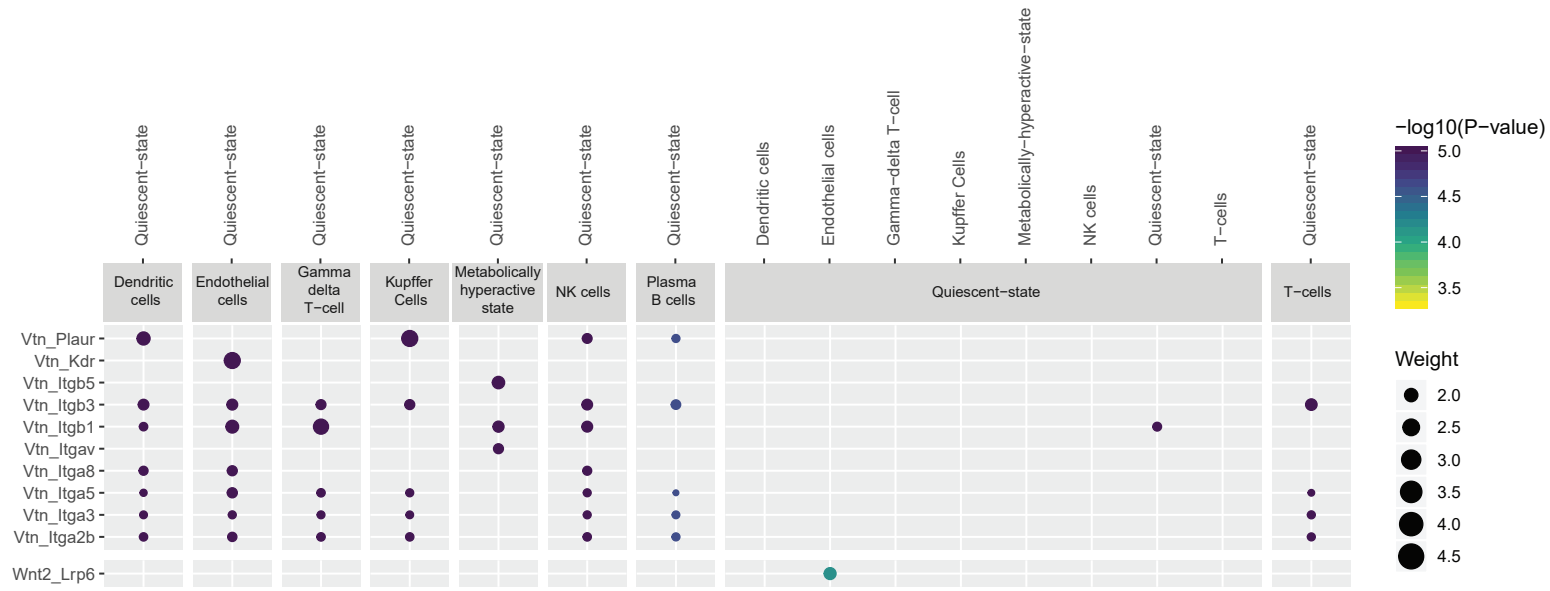


Supplemental\_Fig\_S18:  
Adult\_Ligand\_receptor\_interactions

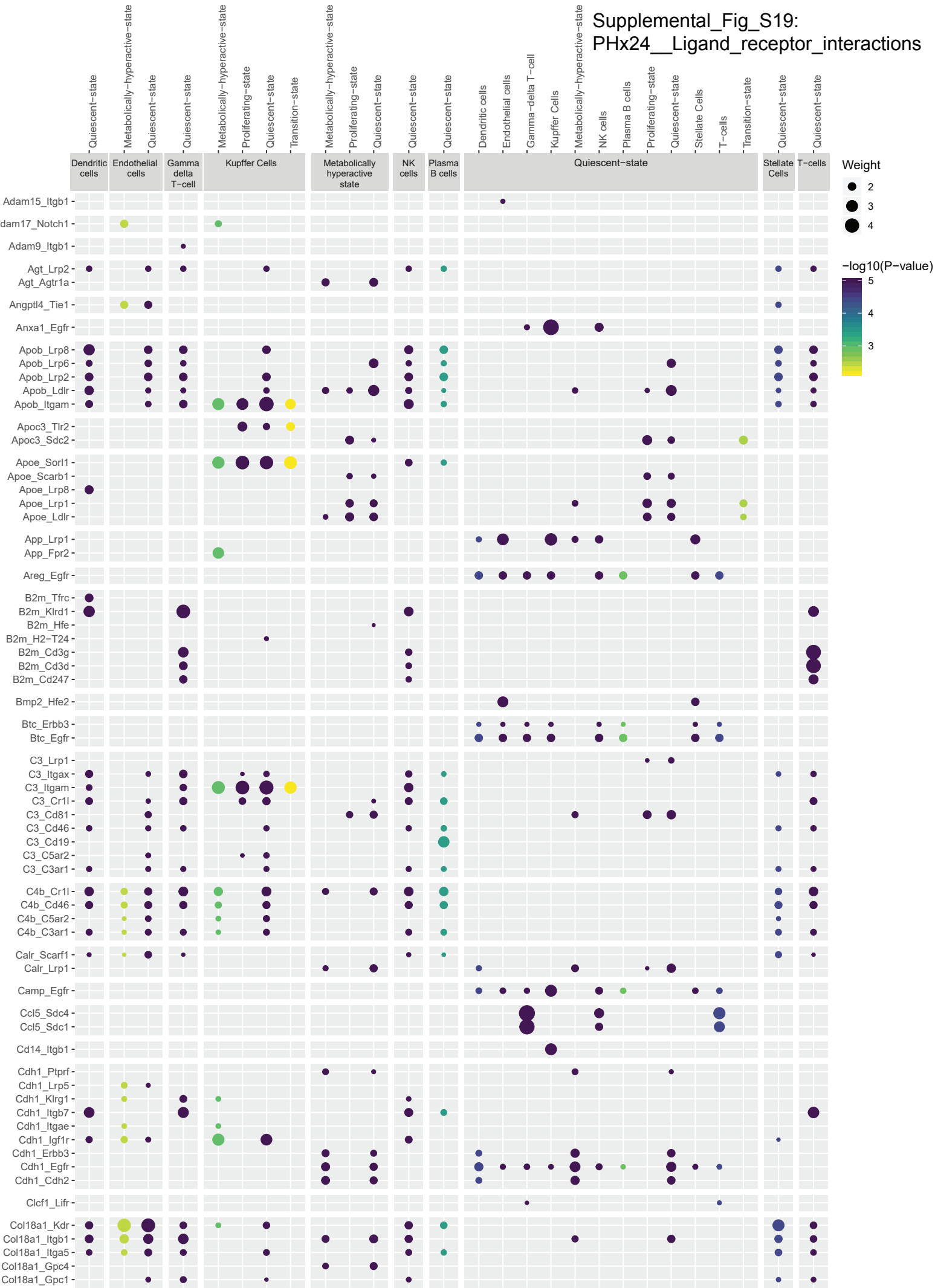


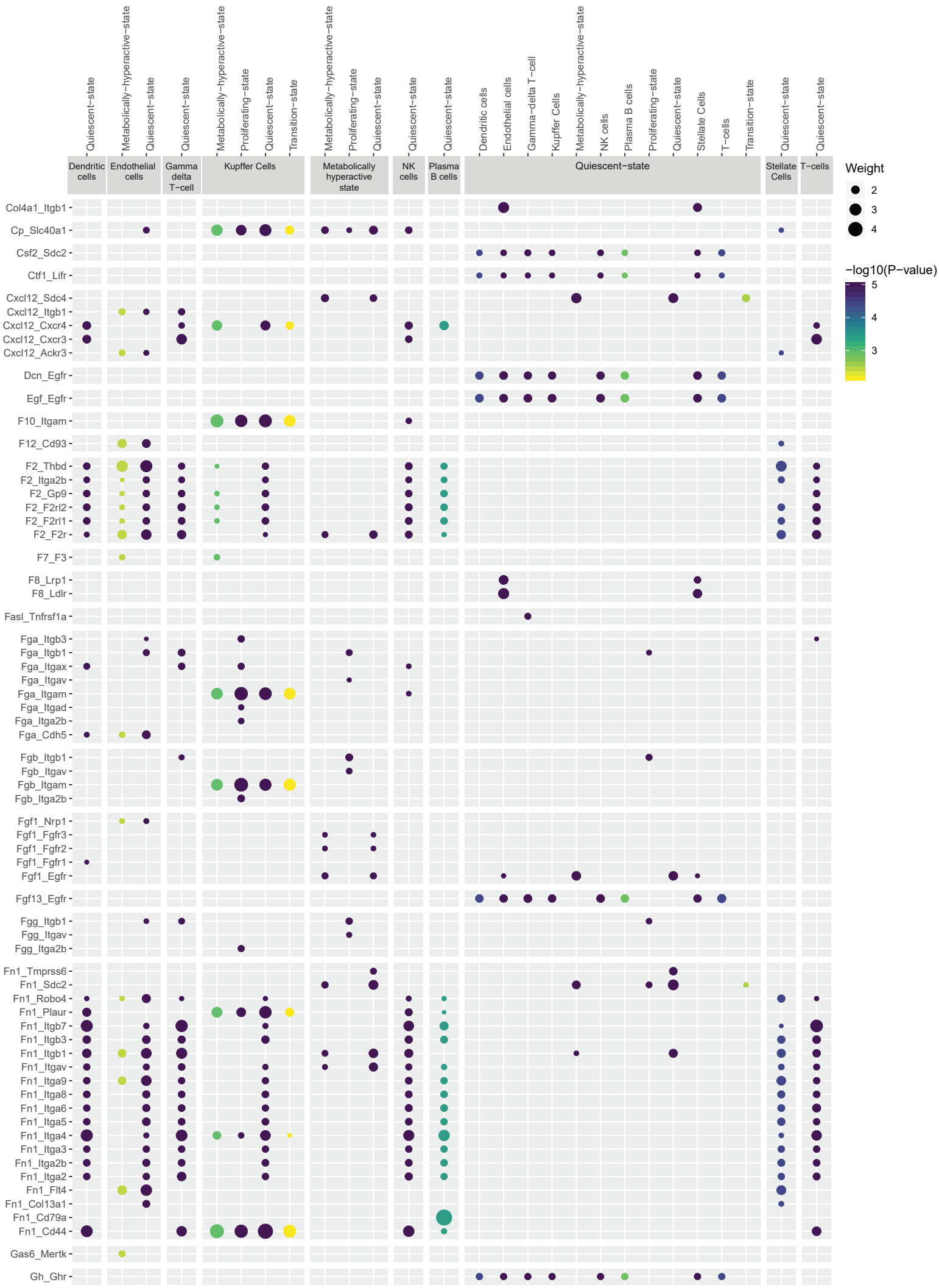


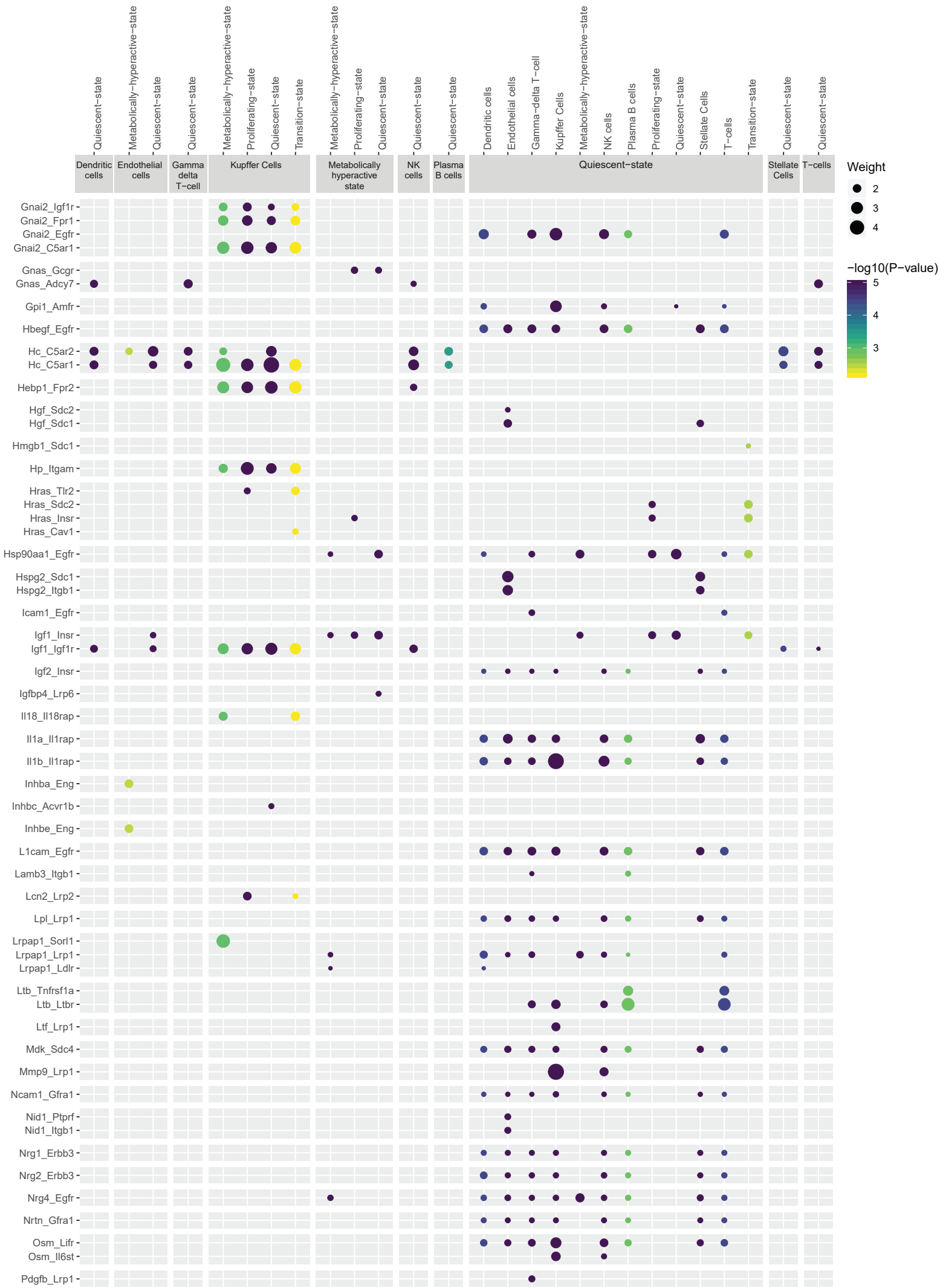


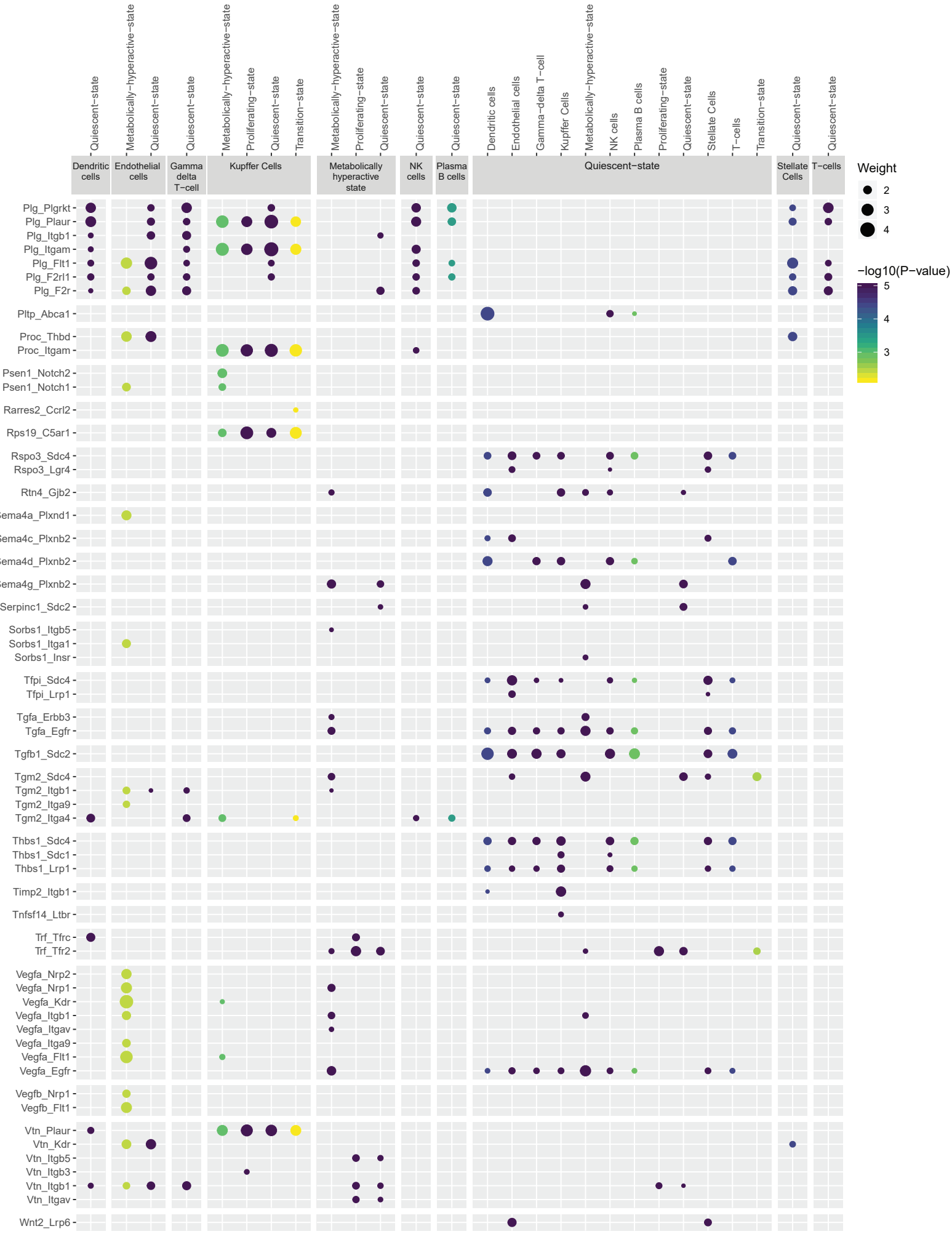


## Supplemental\_Fig\_S19: PHx24\_\_Ligand\_receptor\_interactions

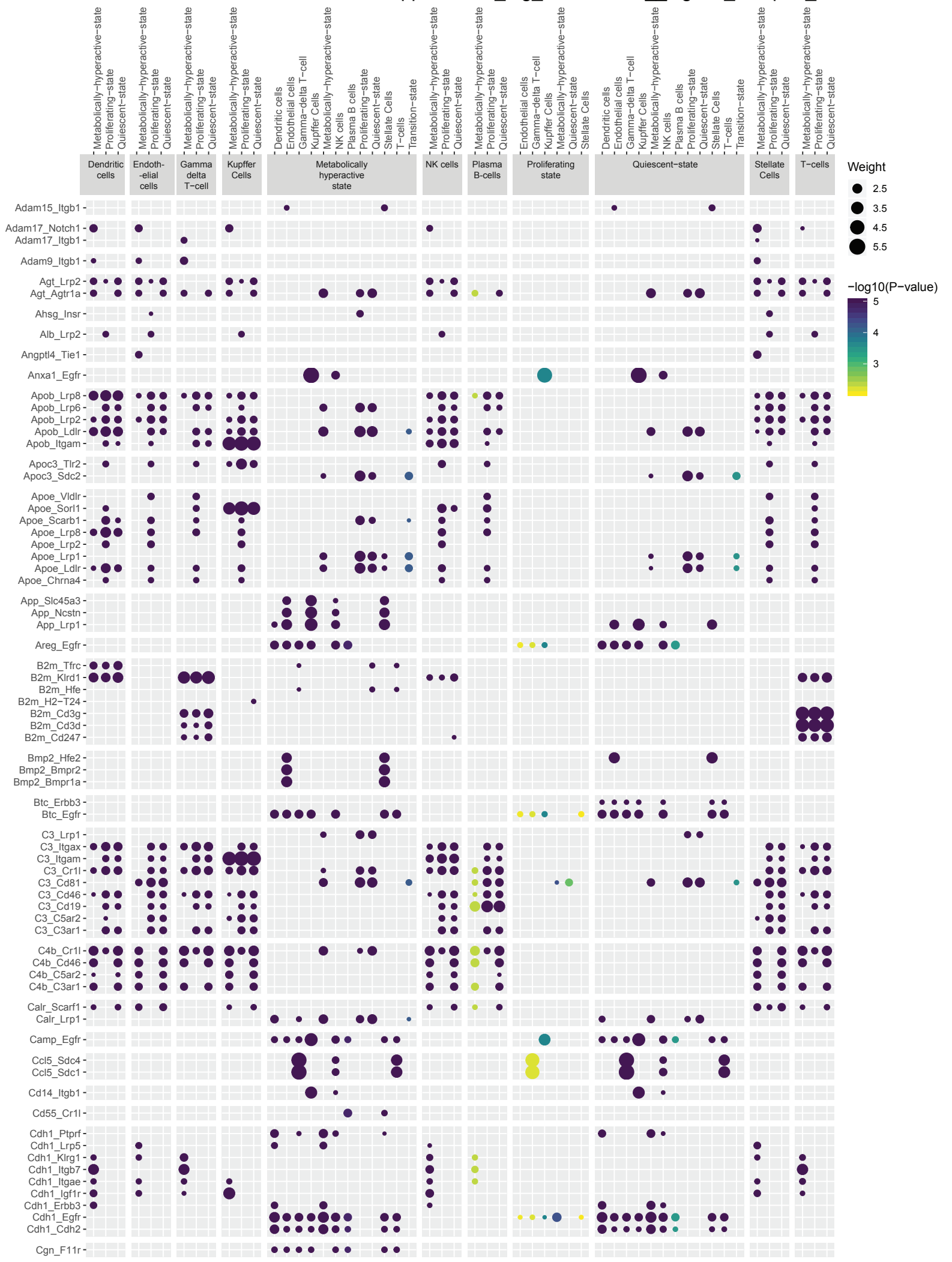


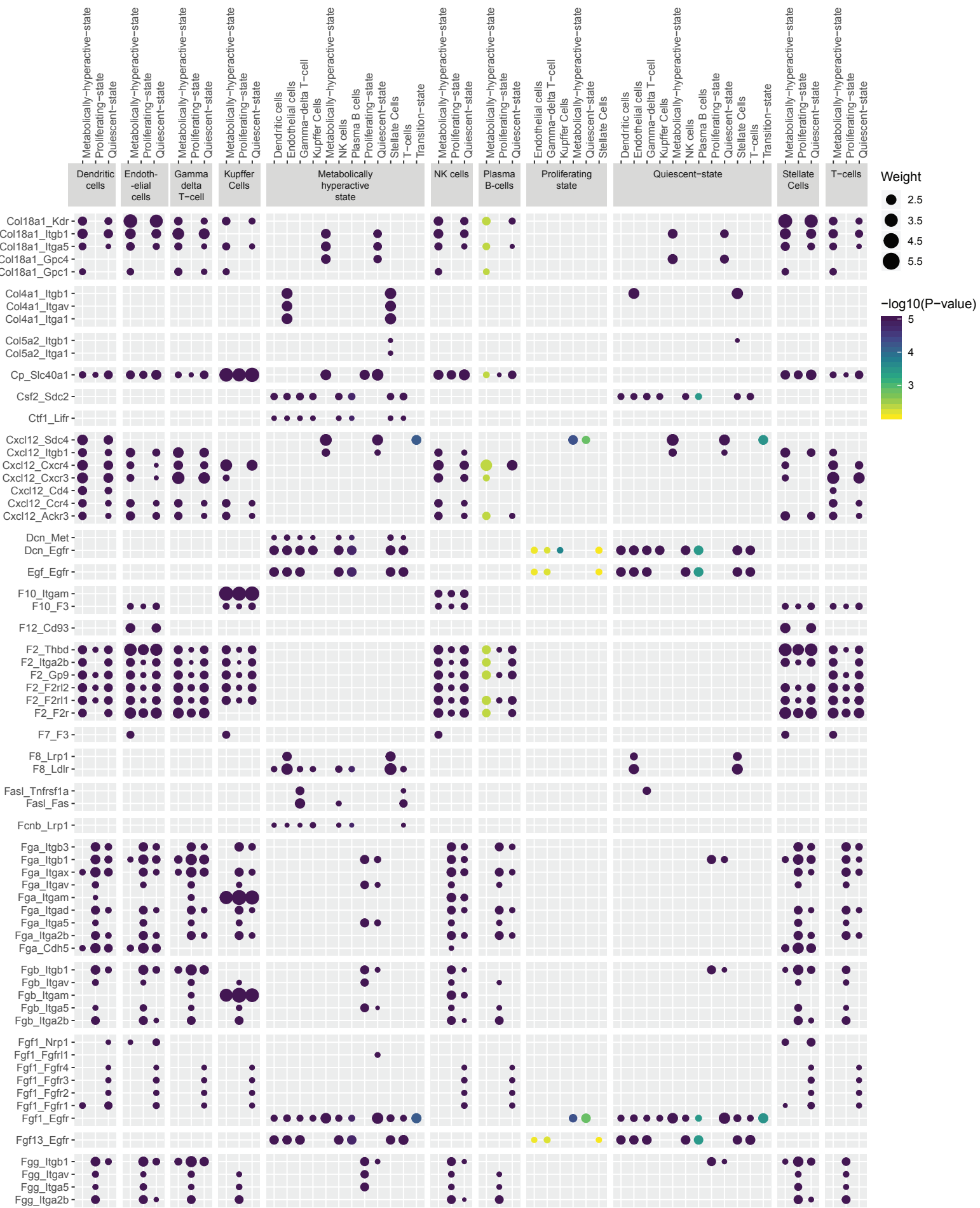


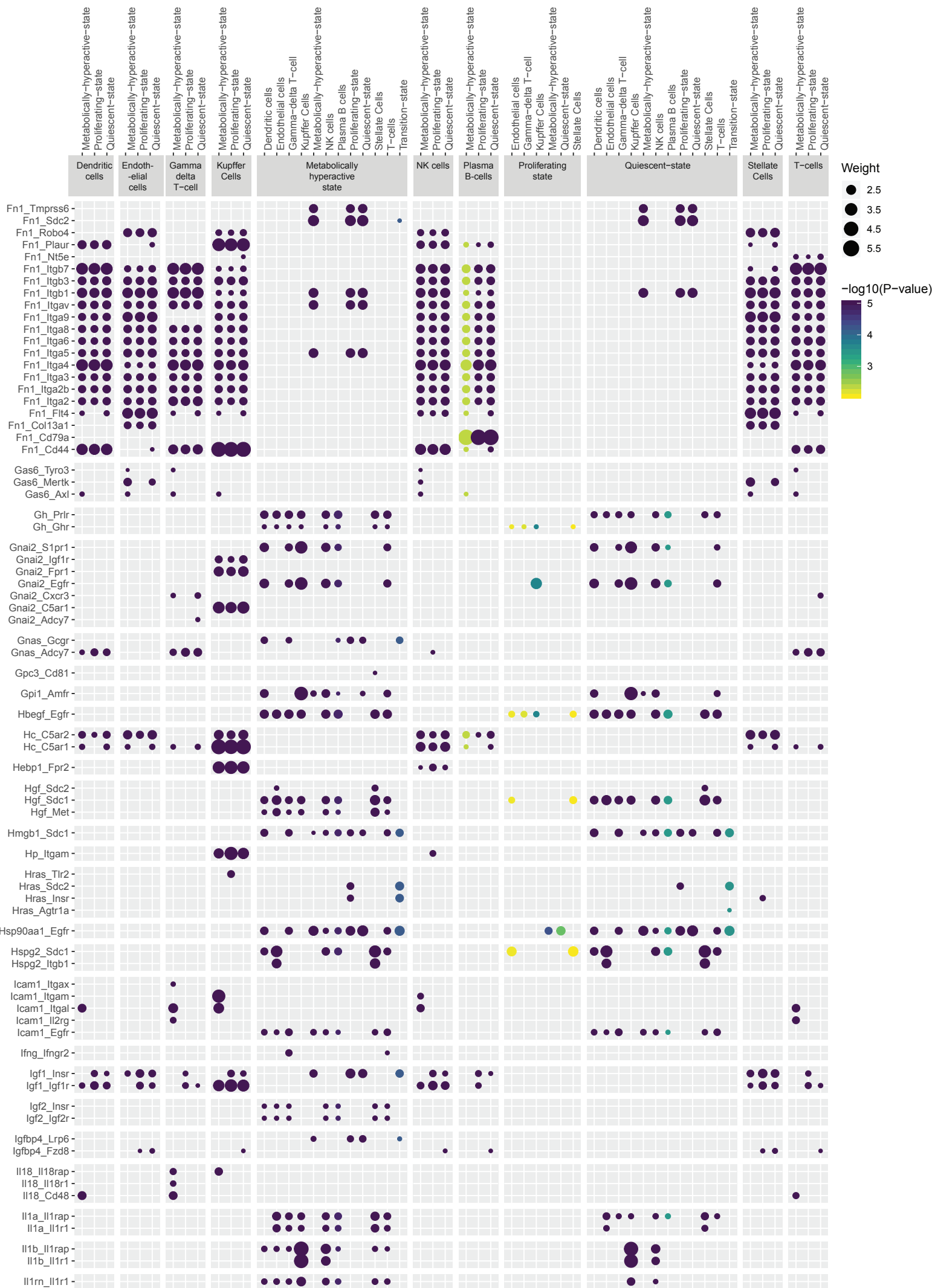


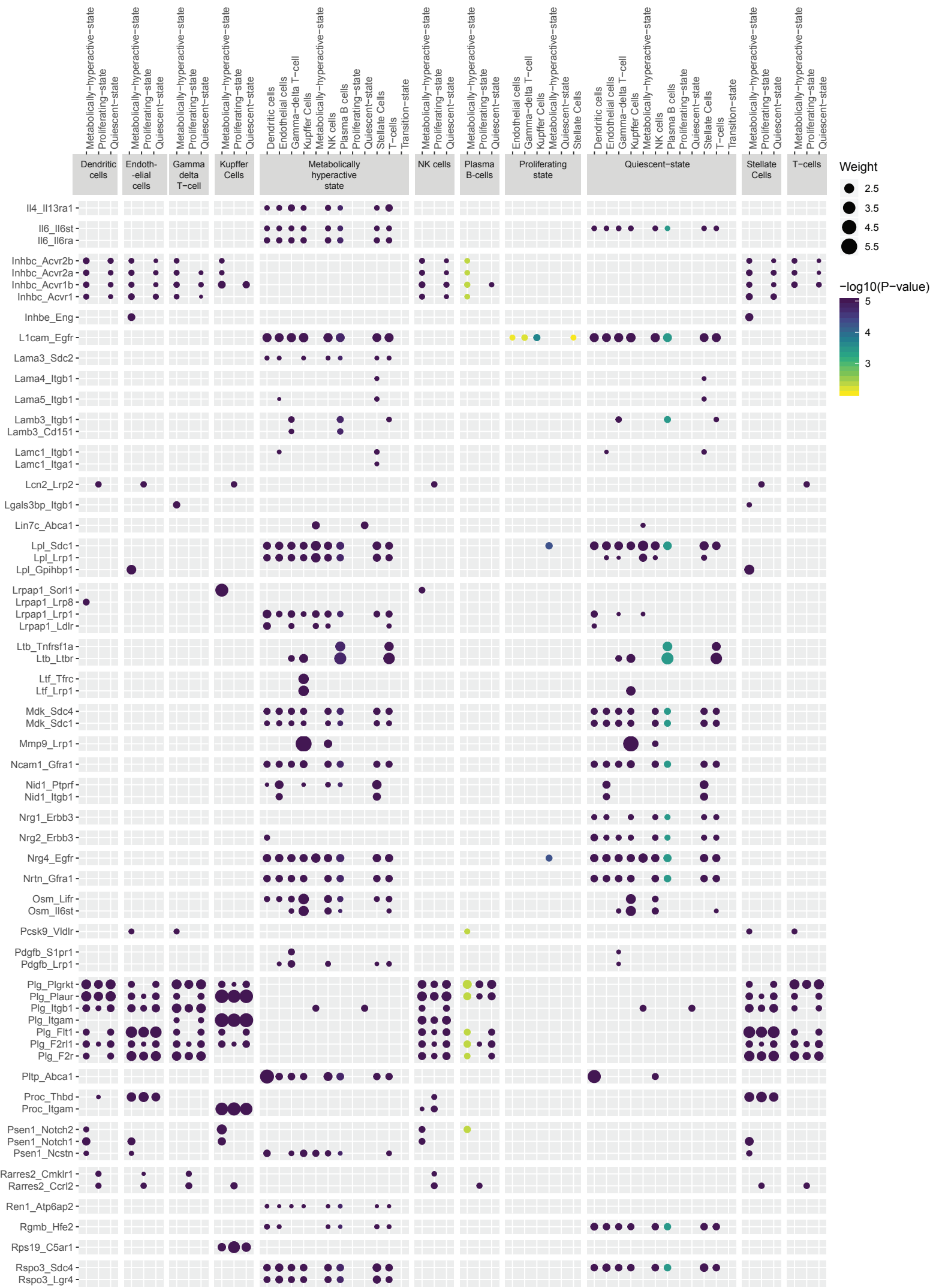


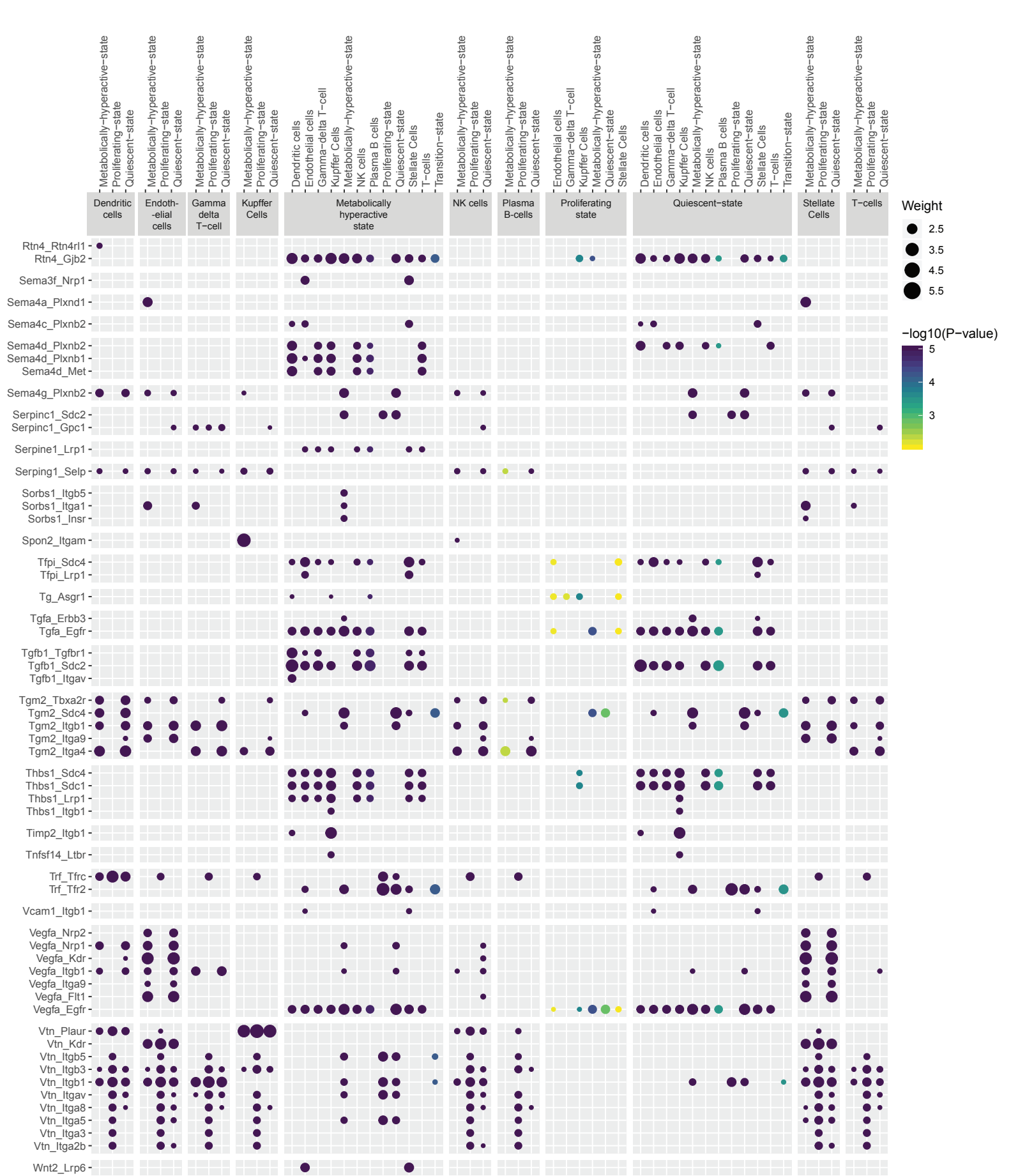
Supplemental\_Fig\_S20: PHx48\_Ligand\_receptor\_interactions











Supplemental\_Fig\_S21: PHx96\_Ligand\_receptor\_interactions

